5-1999

Cut Mark Classification With Energy Dispersive X-ray Analysis

Jennifer Cheryl Love
University of Tennessee, Knoxville

To the Graduate Council:

I am submitting herewith a thesis written by Jennifer Cheryl Love entitled "Cut Mark Classification With Energy Dispersive X-ray Analysis." I have examined the final electronic copy of this thesis for form and content and recommend that it be accepted in partial fulfillment of the requirements for the degree of Master of Arts, with a major in Anthropology.

Murray K. Marks, Major Professor

We have read this thesis and recommend its acceptance:

William M. Bass, Michael Elam

Accepted for the Council:
Carolyn R. Hodges

Vice Provost and Dean of the Graduate School

(Original signatures are on file with official student records.)

To the Graduate Council:

I am submitting herewith a thesis written by Jennifer Cheryl Love entitled "Cut Mark Classification Using Energy Dispersive X-ray Analysis." I have examined the final copy of this thesis for form and content and recommend that it be accepted in partial fulfillment of the requirements for the degree of Master of Arts, with a major in Anthropology.

Murray K. Marks, Major Professor

We have read this thesis and recommend its acceptance:

Accepted for the Council:

Associate Vice Chancellor and
Dean of the Graduate School

CUT MARK CLASSIFICATION WITH ENERGY DISPERSIVE X-RAY ANALYSIS

A Thesis
Presented for the
Master of Arts
Degree
The University of Tennessee, Knoxville

Jennifer Cheryl Love
May 1999

To my family,

George, Cheryl, Seen, Jarrett and Dean.

Acknowledgement

There are several people who made this project possible and I would like to thank them. First and foremost, I will mention my committee members. Dr. Murray K. Marks guided me in defining a specific, approachable question, helped me develop a test design to answer the question, and saw that the project received the necessary funding from the University of Tennessee Anthropology Forensic Center. He also presented me with an opportunity to work as a graduate research assistant in the Department of Oral and Maxillofacial Surgery at the University of Tennessee Medical Center which granted me irreplaceable knowledge and experience. Dr. Michael Elam shared his enthusiasm for electron and ion microscopy while teaching me the complex theory behind them. He also led me to the appropriate statistical test and helped me form questions for future research. Dr. William Bass gave his expertise gained from years of forensic investigation, validating my belief that a more advance method of cut mark classification needed to be developed. He also provided financial support for the purchase of the pigs and the analytical expenses through the University of Tennessee Anthropology Forensic Center.

Furthermore, Dr. David Gerard gave me the idea that developed into this project. He also granted me the opportunity to gain experience that could not be obtained in the classroom by employing me as his research assistant through the Department of Oral and Maxillofacial Surgery at the University of Tennessee Medical Center. Dr. David Joy took the time to teach me how to operate the ESEM/EDX, then had the confidence to allow me to work alone. Bret Brunson, as the supervisor of Dr. David Gerard's electron

microscopy laboratory, provided me with the laboratory equipment and chemicals needed for this study. Derek Benedix assisted me with performing the experiment. Finally, my family and friends gave me continuous support and encouragement. Every individual mentioned played a crucial role in this project and for that I am grateful.

Abstract

Cut marks are preserved records of human activity and are used by anthropologists for a variety of purposes including reconstructing past events. Presently, examination of surface modifications with a dissecting or scanning electron microscope is the most common technique for mark classification. Although appropriate for morphologically typical marks, these methods are subjective and non-applicable to atypical marks. In light of these limitations, the author attempted to develop a method that utilized residual material transferred from a weapon to the bone for classification.

Recent advancements in electron microscopy led to the development of the environmental scanning electron microscope (ESEM) equipped with energy dispersive X-ray analysis (EDX). Analytical capabilities of this microscope include identifying the elemental composition of the surface of fresh bone. In the study, this instrument was used to compare the elemental composition within a cut mark to the elemental composition of an unmarked control area.

The cut marks analyzed in the study were the result of stabbing intravenously euthanized domestic pigs (*sus scrofa)* with smooth, slightly serrated, and serrated edged knives. The experiment was designed to mimic a forensic event, from stabbing the pigs to leaving them in an open-aired, wooded facility to decompose. Each bone inflicted with a cut mark was collected, washed with ethanol and analyzed with an Emas/Mas SEM equipped with a EDX Robinson Detector. The results on the analysis were statistically evaluated with the *t*-test and *chi*-square test using SAS v6.12 statistical program.

Analytical results showed that significantly more carbon was present in the cut marks made with slightly serrated and smooth edged knives than on their respective control surfaces. However, Iron (Fe) and chromium (Cr) which makes up a larger percentage of the composition of stainless steel ($\geq$83.03% and 13%, respectively) than C (.25%), was not detected in any of the marks. The differences in the amounts of C are more likely an artifact of analysis than residual material. Possible reasons for the results include the limitations of EDX when applied to trace elemental analysis of rough surface specimens (such as bone) and the critical quantity of an element needed for detection. Hence, cut mark classification is not possible with EDX given current limitations of the instrument. However, refinements in electron and ion microscopy will overcome the present limitations making future development of a cut mark classification method based on residual material foreseeable.

Table of Contents

List of Figures

Figure **Page**

Chapter 1

Introduction

Cut marks on bones are preserved records of human actions and are thus, invaluable to many subdisciplines of anthropology including paleoanthropology, archaeology and forensics. Research founded on cut mark classification ranges from evidence of early hominid neurological development (Shipman and Rose 1983; Bromage and Boyde 1984) to the interpretation of trauma in recent forensic cases (Frayer and Bridgens 1985). Despite the significance of cut marks, current analytical methods are rudimentary. However, advancements in other fields, such as electron microscopy, provide opportunities to develop more sophisticated analytical techniques.

Brief Summary of Cut Mark Based Research in Paleoanthropology and Archaeology

Bone, a highly mineralized tissue, withstands pre and postdepositional processes longer than soft tissue. Cultural alterations to bone from activities such as butchering, funeral practices and violence are recorded on and preserved with it. Using the evidence of these alterations, anthropologists attempt to reconstruct human activities.

Shipman and Rose (1983) state that establishing directionality of cut marks on animal skeletal remains from early hominid sites would constitutes proof of handedness among early hominids. They continue by equating handedness with brain laterality and consequently, the specialization of the two hemispheres of the brain for different tasks. Such neural development marks a significant evolutionarily advancement of the human

brain. However, they fail to establish a criterion for determining directionality. Responding to Shipman and Rose (1983), Bromage and Boyde (1984) analyzed 210 experimental cut marks made with flint and obsidian unretouched flakes and found that oblique faulting (Figure 1) is consistently present on the medial wall of a cut mark, with respect to the operator. They propose that the faulting is the result of slight supination of the hand despite attempts to keep the tool perpendicular to the bone and conclude that directionality of a cut mark is determinable.

White (1986) discovers that cut marks on the cranial vault and infra-orbital surface of the Middle Pleistocene Bodo cranium from Ethiopia closely resemble experimental cut marks made by stone tools on fresh bone (Figure 2). The resemblance of the marks suggests intentional defleshing of an individual and is indicative of early hominid mortuary practices and possible cannibalism.

Owsley (1994) outlines the pattern of warfare among the Northern Plain Indians, from the Prehistoric to the Disorganized Coalescent period (circa 1600-1832), with evidence of scalping on 751 crania of individuals from 15 archaeological sites. Scalping, the incising of the skin over the skull with a sharp instrument to remove the soft tissue (Hamperl 1967), frequently leaves cut marks on the cranial vault. From the cut marks, Owsley (1994) identifies victims, extent of warfare, proximity of the violence to a village, and the arrival of an additional Indian group to the region.

In sum, the previous examples illustrate the weight of cut mark classification in paleoantrropological and archaeological research. Mark classification and interpretation has shown to play a significant role in reconstruction human behavior at all levels of

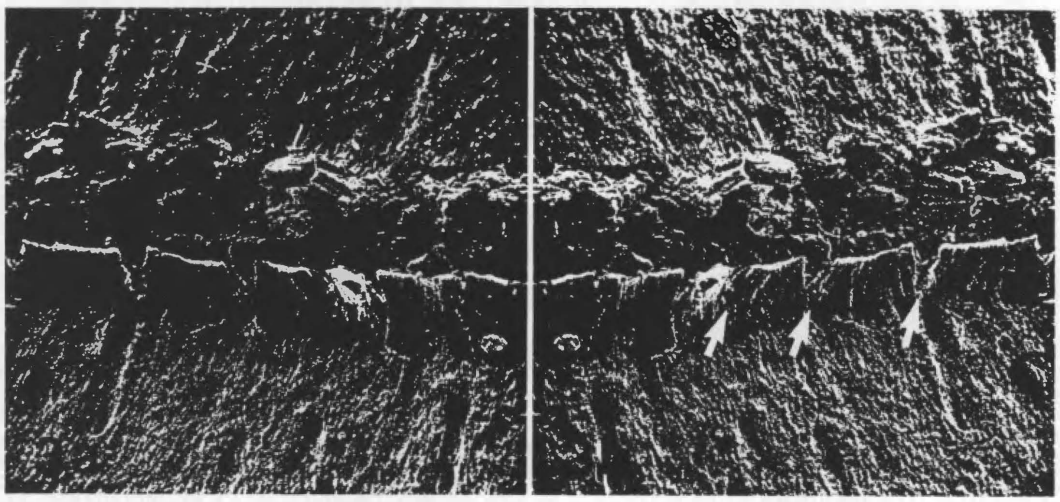

Figure 1. Mirror image of a cut mark, arrows mark oblique falter. Field width = 950μm (Bromage and Boyde 1984: 362).

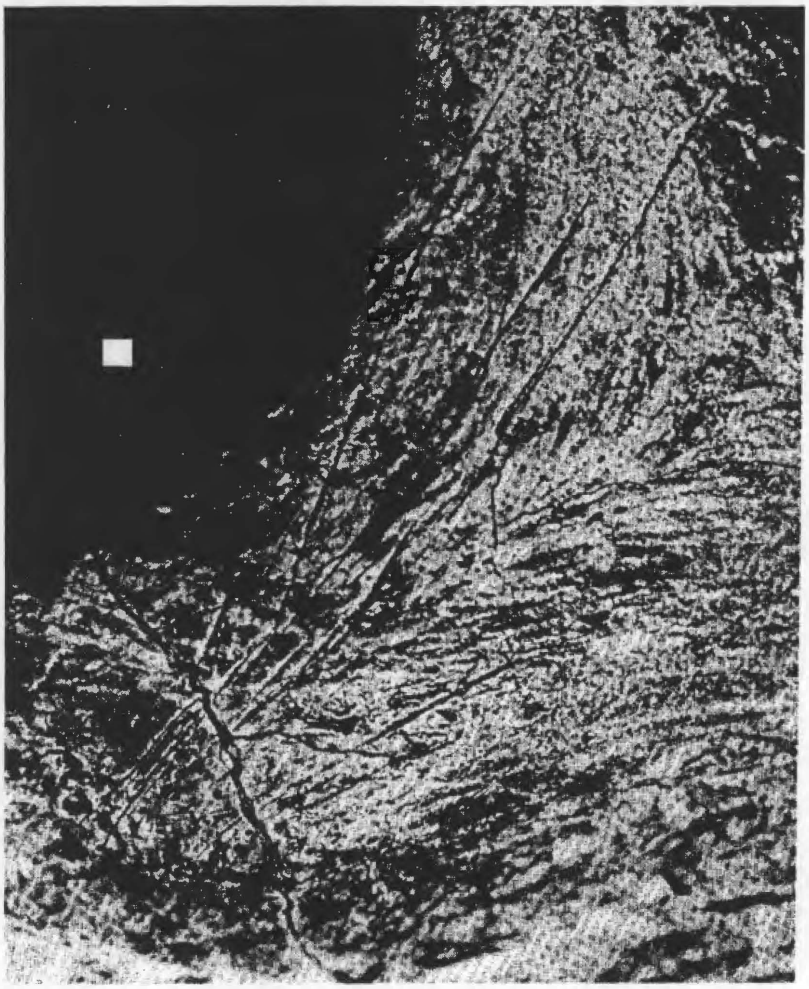

Figure 2. Cut marks found on the left malar bone of the Bodo cranium. Scale bar represents 1.0mm. (White 1986: 506)

organization, from the early hominid hunter to regional warfare. Furthermore, the temporal depth to which it is applicable is infinite.

Brief summary of the Role of Cut Marks in Forensic Anthropology

A forensic case raises many questions including the identity of the individual, estimating the time since death and establishing cause and manner of death (Sauer 1984). Identification of individuals and estimating time since death are areas outside the scope of this thesis, but cut mark classification is directly linked to the cause and manner of death. Forensic cases include individuals in all stages of decomposition, from nearly undetectable to completely skeletonized. The longer the post mortem interval (PMI), the time between death and discovery, the more difficult the task of answering the previously posed questions. Cause of death refers to a mortal interruption to a physiological system of the body that results in death (Adelson 1974) and is usually established from a soft tissue examination by a physician. As the decomposition process of the soft tissue advances the cause of death becomes obscured. Once it is completely undeterminable, only a manner of death can be suggested. Manner of death characterizes the circumstances surrounding the death and includes five categories: accidental, natural, suicide, homicide and unknown (Spitz and Fisher 1980; Morse 1983; Sauer 1984). Forensic anthropologists with limited access to the history of the victim and crime scene analysis are not qualified to estimate a manner of death, but can contribute to the investigation by observing and reporting osseous anomalies.

Sauer (1984) dissected and macerated partially skeletonized remains of an adult male to examine the bones for signs of perimortem trauma. Previously, a medical

examiner had examined the remains and reported that he found no evidence for cause or manner of death. In addition to comminuted fractures of the apex of the mastoid process resulting from lateral blunt force trauma to the head, Sauer identified small cut marks on opposing borders of two adjacent ribs (Figure 3). The more superior of the two marks was a notch on the inferior border of the second left rib. The notch had a flat base suggesting a crushing force accompanied the incision. The more inferior mark was located on the superior border of the third left rib. The morphology of the mark represented a slicing of the bone with a sharp instrument. The investigator concluded and was later confirmed by eyewitness accounts that the cause of the two marks was a single blow to the chest. The slice was inflicted with the sharp edge of the knife and the notch was the result of a compression force received from the flat back edge of the knife. Based on the skeletal evidence and the eyewitness accounts, Sauer testified that the manner of death was homicide. However, Sauer stated that "[h]ad there been no witness to the crime, then it seems unlikely that the marks detected on the skeleton would have been sufficient grounds to establish manner of death" (1983: 182).

In addition to simply representing sharp force trauma, cut marks, specifically saw marks, record class characteristics which identify saw size, type, shape and power source (Symes et. al. 1998). There are three types of saw marks common to bone: false start scratches, false start kerfs and complete sectioned cuts. A false start scratch, the most superficial of the three mark types, does not record much information and is often mistaken for a knife cut mark. A kerf forms when a saw's teeth cut into the bone and includes several diagnostic components. A complete cut is a kerf that continues through the bone with the floor of the kerf retained as breakaway spurs (Figure 4) (Symes et. al.

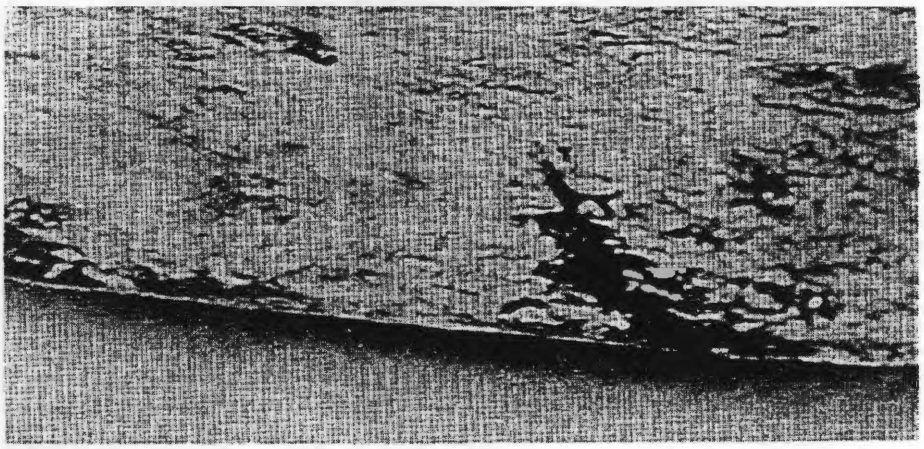

A

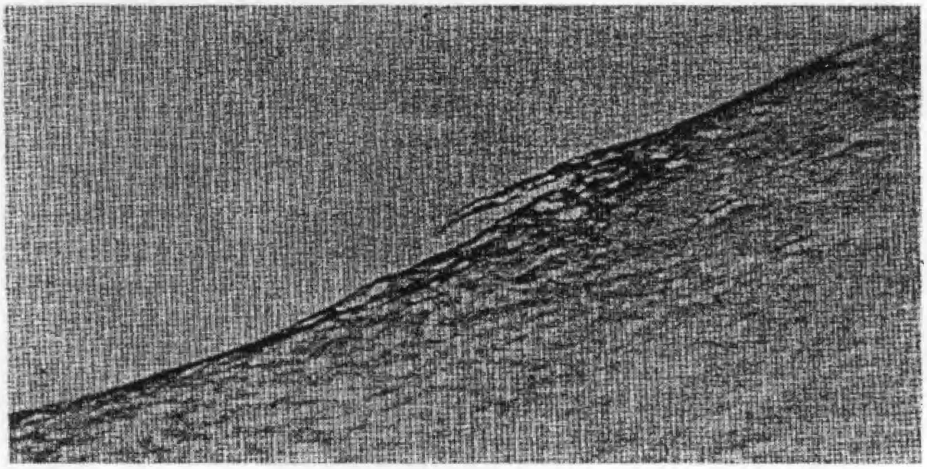

B

Figure 3. Cut marks located on adjacent ribs. A is result of contact with the blunt edge of the knife and B is the result of contact with the sharp edge of the knife (Sauer 1984: 180).

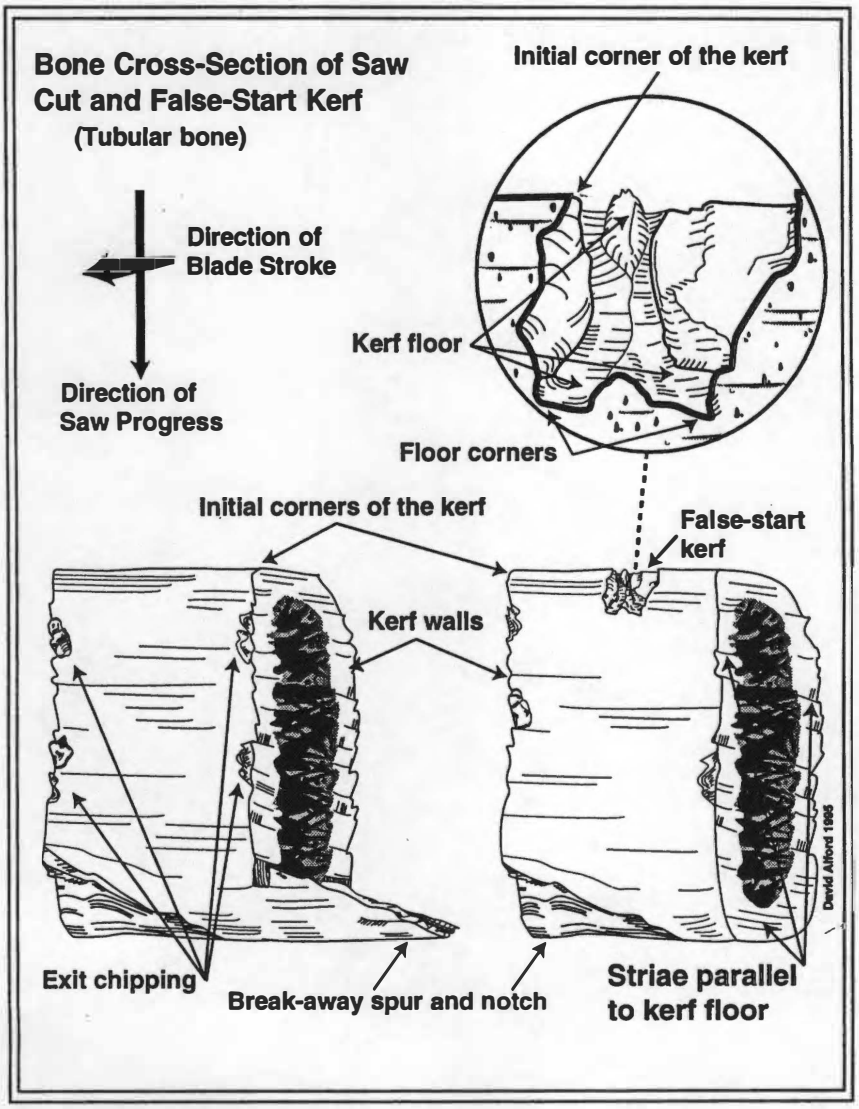

Figure 4. Illustration of a false start kerf, kerf walls, exit chippings, stria and break-away spur seen in saw marks. (Symes et al. 1998: 399).

1998). The kerf floor of false starts and breakaway spurs of a complete cut record the most information about the point of each tooth and their spatial relationship to one another. Details about the sides of the teeth and the blade movement are recorded in the striae of the kerf walls. The tooth pattern is retained in the first and final strokes of the saw, which are not obliterated by following strokes. The wave formation, used to calculate teeth per unit of distance, and the swarf lips, used to determine the direction of a cut, are documented in the tooth pattern (Figure 5) (Andahl 1978).

Numerous specimens of cut bone from the dismembered remains of 14-year-old female were brought to Dr. Steve Symes, a forensic anthropologist, for examination. The remains were found in the St. Catherines area of Ontario, Canada, and were believed to be the work of a serial killer active in the area. Initial examination revealed that all marks were similar and Symes concluded that they were made with the single class of saw (Symes et al. 1998). The uniformity of the cuts, lack of entrance or exit chipping, and polished and wide kerf shapes indicated a powered saw. Furthermore, the circular pattern with a fixed radius found in the striae of the kerf wall indicating a powered circular saw. Nearly a year after the young girl was abducted a second victim was discovered, a 15 year old female also from the St. Catherines area. The second victim's abduction mirrored that of the first, but the body was not dismembered. Symes was subpoenaed to testify on the class of saw used to dismember the victim. He testified that the markings on the bones were consistent with marking made by a powered circular saw. Although professing his innocence, the suspect admitted to using a McGraw-Edison circular saw, which is capable of producing marks similar to those in question. The suspect was convicted of first-degree murder.

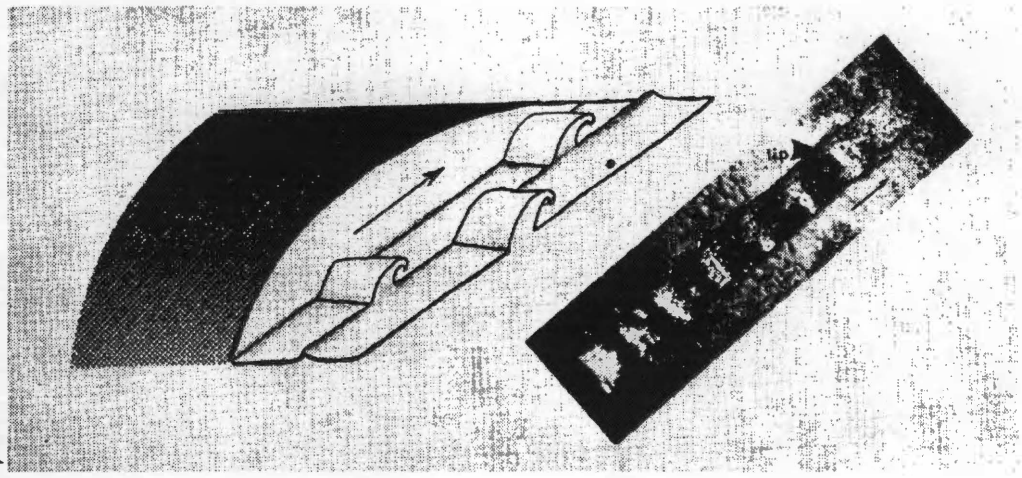

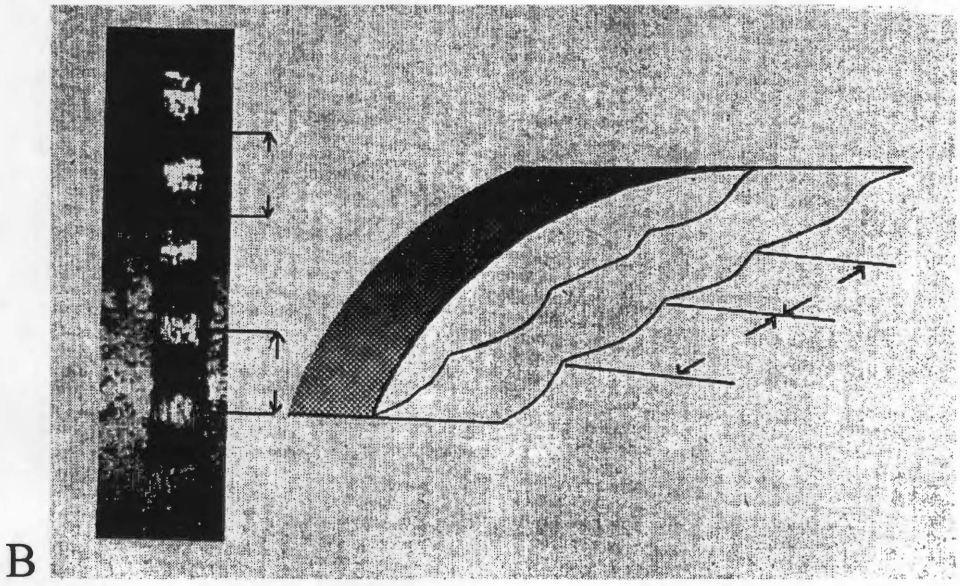

Figure 5. Illustration of A) swarf lips and B) wave formation (Andahl 1978: 37-38).

Reichs (1998) reports a case in which two dismembered bodies were found in several athletic and plastic bags dispersed around Ste-Adele, Quebec. Bone fragments containing the cut marks, the left and right radii, ulnae, femora, tibiae and fibulae and two cervical vertebrae, were extracted from the skeletal remains. Microscopic and gross analysis revealed that a saw and knife were used for dismemberment. The knife marks were found in association with the saw marks located on the long bones and without accompanying saw marks on the cervical vertebrae. The cut marks cluttered around the saw mark overlaid the false starts and paralleled and participated in the breakaway spurs. Examination of the saw mark suggested the saw was an eight to ten tooth per inch (TPI) handsaw with chisel teeth. This case remains unsolved.

The previous examples illustrate the value of cut marks to forensic cases and that they occasionally play a role in conviction of a suspect. The examples also outline the greater amount of information recorded by saw marks than by knife marks. The repetitive action used to generate a saw mark leads to a more conspicuous mark, which is less likely to be overlooked or mistaken for a non cut mark anomaly.

Methods of Cut Mark Analysis

Cut marks can be divided into two categories: repetitive action; and single action. Repetitive action marks result from a hand or powered saw as the tool removes increasing amounts of material from the same site (Symes 1992). Single action marks result from a single blow with a knife or other sharp tool. The continuous actions at a single site makes repetitive action marks more informative then the single action marks.

Sawn surface analysis is a three-step procedure beginning with an examination of the sawn surface. As previously stated the morphology of mark records details about the actions of the operator, blade type and the condition of the teeth. The first step of saw mark analysis includes examinations of false start kerfs and complete cuts. The results identify the saw type used to make the mark. The suspect saw type or suspect saw, if present, is then used to make a test cut. Finally, the two marks are compared and a positive or negative identification of the suspect saw or saw type is made (Andahl 1978; Symes 1992).

In comparison to repetitive action marks, single action marks record very little information. Aside from serrated bladed knives, which imprints the serration pattern on the bone, single action marks can not be used to determine the morphology or blade dimensions. The length of a cut mark, for example, is the result of how far the knife cuts into the material rather than the size of the blade (Symes 1992). Despite the elusiveness of single action marks there are several methods of analysis, i.e., surface and subsurface visual inspection at various magnifications.

Surface analysis is accomplished by magnifying the surface of the mark with a hand held magnifying glass, dissecting microscope or a scanning electron microscope (SEM). The dissecting microscope and magnifying glass require no surface preparation, are nondestructive to the specimen and are cheap, accessible instruments. SEM increases the magnification and resolution possibilities from 400x to 7,000x, but requires a large amount of sample preparation, including meeting dimensional limitations, dehydration and coating the specimen (if not using an Environmental-SEM). In order to preserve the

specimen, analysts often use replicas. However, replicas fail to retain the detail of the original specimen and generate replication artifacts (Rose 1983).

Drawing with a diamond-tipped stylus and thin sectioning of a replica are the subsurface analytic techniques used to investigate the vertical dimensions of cut marks. The diamond tip of the stylus is two nanometers (nm) in diameter and falls into the crevice as the instrumental arm pulls it back and forth over the scored surface. The instrument converts the vertical movement into electrical signals. It measures and translates the signals into a two-dimensional schematic diagram that illustrates the vertical extension and topography of the cut (Figure 6). This method does not require surface preparations and the size of the object can vary greatly. It also generates numerical data from a three-dimensional structure (During and Nilsson 1991).

Transverse sectioning of a cut mark replica also provides a view of the vertical profile of the cut mark. This method, developed by Walker and Long (1977), includes making a polyvinyl replica of a cut mark and sectioning it into five millimeters (mm) thick sections. The thin sections produce a serial view of the morphology of the cut mark and permits the comparison of the width of the mark, the straightness of the walls, the sharpness of the point and the depth of penetration (Figure 7).

The weakness of morphologically based techniques for cut mark classification is the lack of an alternative method to verify the results. Cut mark mimics, such as bone anomalies and surface modifications, compromise the accuracy of these methods. Partially fused epiphysis, irregularly developed flat bone, anomalous bony structure and vascular grooves are biological agents that can erroneously suggest perimortem trauma (Sauer 1984). Furthermore, several researchers (Potts and Shipman 1981; Shipman and

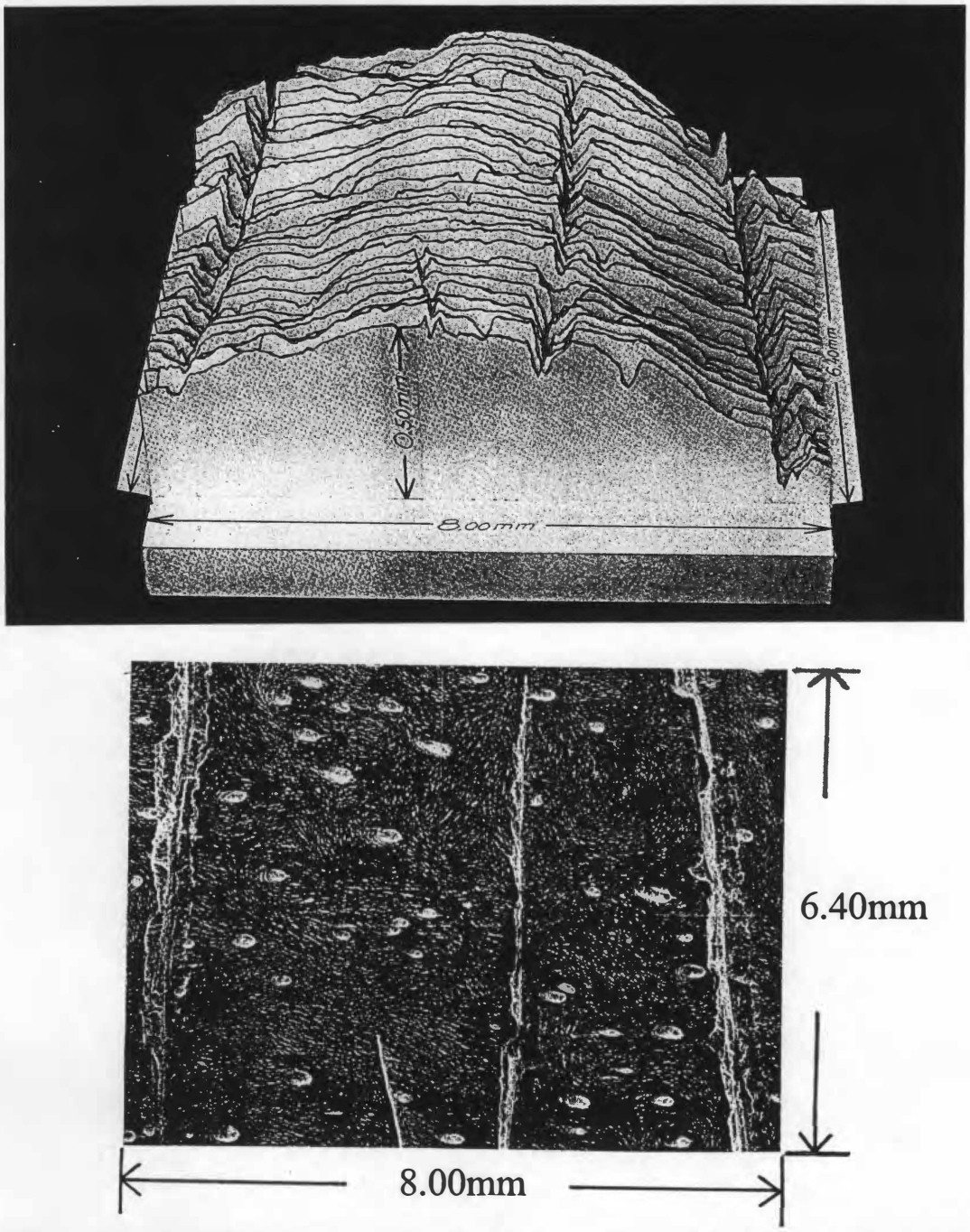

Figure 6. Top image is a model constructed from the diamond tip analysis of cut marks found on the frontal bone of a Neolithic cranium. Bottom image is the same area viewed with a SEM microscope (Durring and Nilsson 1991: 120).

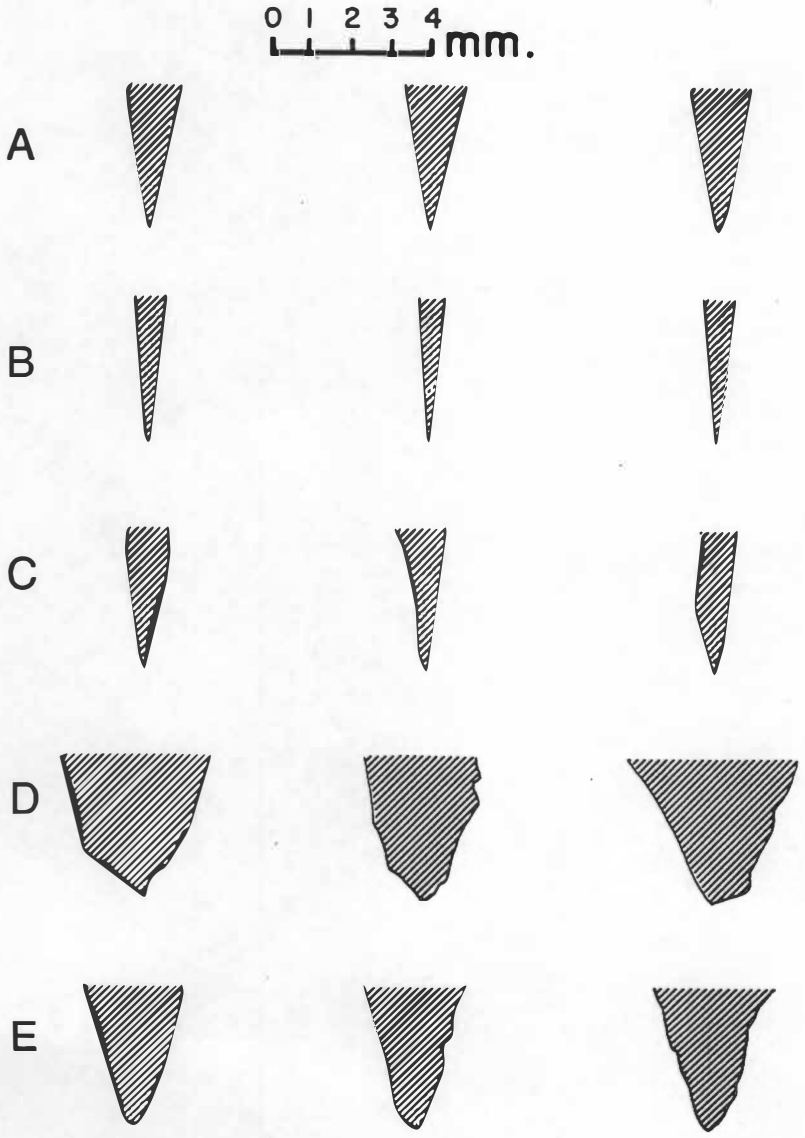

Figure 7. Tracings of enlarged photographs of traverse sections made at 5mm intervals, A) steel hand axe, B) steel knife, C) obsidian knife, D) and E) bifacially flaked tools (Walker and Long 1977: 607).

Rose 1983; Andrews and Cook 1985; Behrensmeyer et. al. 1986; Olsen and Shipman 1988; Blumenschine and Selvaggio 1988; Shipman 1988; Fiorillo 1989; and White 1992) have cautioned about pseudo-cut marks resulting from post-depositional processes, such as carnivore and rodent activity, root etching, trampling, and weathering. Pseudo cut marks are mistaken as cut marks and vis a versa at all levels of magnification. For example, SEM based criteria established as diagnostic for human-induced cut mark has been shown to be faulty (White 1992).

Blumenschine et al. (1996) tested the accuracy of visual analytical methods of mark classification. The test design required novices with only three hours of training to identify bone surface modifications and match them to the effector. The novice used hand held magnifying glasses and low-powered microscopes to analyze the marks. The investigators inflicted the experimental marks in the bone with carnivore teeth, hammerstone percussion, and metal knives. Blumenschine et al. (1996) reports that the novices identified the marks and matched them to the effector with 86% accuracy. The experiment was repeated with the same individuals after they received an additional three hours of training. They increased their accuracy of mark identifications and effector matching to 95%. Blumenshine et al. (1996) concluded that published caution of the dangers of mimics of cut marks, percussion marks, and carnivore tooth marks are overstated. In addition, they state that hand held lens and low-powered dissecting microscopes are sufficient instruments for analysis of cut marks, implying the use of SEM as unnecessary.

Although Blumenshine et al. (1996) make a valid observation, they are concerned with the accuracy of analyzing archaeological and paleoanthropological specimens.

Unlike forensic anthropological specimens, archaeological and paleoanthropological specimens are not involved in murder trial; therefore, are not under the scrutiny of the court system. The medico-legal field's interests in cut marks that reflect perimortem trauma of recently deceased individuals demands more quantitative methods for classifying marks. Therefore, a technique that is based on a characteristic of cut mark beyond morphology is needed to reach higher levels of confidence.

In response to the demand, this study asks whether cut marks are classifiable from residual material transferred from the weapon to the mark during mark infliction. The material of modern knives is usually stainless steel. The elemental composition of stainless steel includes iron, carbon, manganese, silicon, chromium, nickel, molybdenum, nitrogen, thallium, and niobium (Brandes and Brooks 1992). The inorganic matrix of bone is mainly composed of calcium and phosphorus, but also includes bicarbonate (C_2O_6), magnesium, potassium, and sodium (Junqueiral et al. 1995). Given the differences in elemental composition of stainless steel and bone, it is hypothesized that if residual material common to stainless steel is present in the mark, the mark is most likely the result of sharp force trauma opposed to biological agents or post-depositional processes.

Chapter Two

Instrumentation

Advancements in microscopy led to the development of the electron probe microanalyzer (EPMA) followed by the ion probe microanalyzer (IPMA). The capabilities of both instruments include elemental analysis; however, EPMA is applicability to biological specimens, while IPMA is not. Additionally, the development of the environmental scanning electron microscope (ESEM) furthers the suitability of electron probe microanalysis to biological samples. This chapter outlines the history, application, and limitations of the two instruments, with a detailed review of energy X-ray analysis, the instrumental mode used in this study.

Electron Probe Microanalyzer

History

Electron probe microanalyzer results from developments in two distinct fields: X-ray spectrochemical analysis and electron microscopy. In the 1940's, scientists united their knowledge of characteristic X-ray wavelengths emitted from an element excited by an energy source with electronic detectors, stable sealed-off X-ray tubes and large crystal analyzer to berth fluorescent X-ray spectroscopy (Birks 1971). The advantage of the X-ray spectrum when compared to visible or ultraviolet spectra is the orderly progression of wavelengths with the increase of atomic number. Furthermore, the emitted X-rays originate from the inner-shells of the atom where the physical state or chemical combination of the element has a minimum effect.

Meanwhile, electron microscopy advanced rapidly from research of radio-frequency power supplies, hot-filament electron guns and focusing properties of electron lenses (Birks 1971). This research led to the construction of a scanning electron microscope that detects then used backscattered electrons to form an electron picture of the specimen surface. Thus the knowledge of electron lens aberrations and corrections developed so that the field was ready for the micron beam-size requirements of the electron probe (Birks 1971).

In 1949, Castaining and Guinier tied the two fields together and reported the conversion of an electrostatic electron microscope to focus an electron beam on a solid specimen and an X-ray spectrometer to measure the characteristic X-ray generated. Several analytical techniques grew from this vantage point including wavelength and energy dispersive X-ray analysis (WDX and EDX, respectively). WDX measures the wavelength of the emitted X-ray, while EDX measures the energy. Both spectrometers give the same information: a spectrum of intensity (number of counts, or counts per unit of time) versus an axis of either energy or wavelength of the X-ray.

Formations of X-rays

The base of WDX and EDX is the emission of characteristic X-rays from the interaction of projected electrons with matter at the atomic shell level (LeFurgey and Ingram 1990). An atomic electron has a specific energy value in an atom, its energy level. Bohr in 1913 (see Ebbing 1996) developed the following formula to derive the energy level of the electron.

$$E = -R_H/n^2 \quad n = 1,2,3\ldots$$

Where R_H is a constant with the value 2.179×10^{-18} Joules (J) and n is the principal quantum number. An electron changes energy by undergoing a transition from one energy level to another energy level. When an electron in a higher energy level undergo a transition to a lower energy level the excess energy is released as an emitted photon or X-ray. The following formula describes the relationship between the energy of the emitted photon and the energy levels of the electron.

$$h\nu = E_i - E_f$$

Where h is Planck's constant with the value of 6.63×10^{-34} J•s (s = seconds), ν frequency of oscillation of the specific solid, E_i is the initial energy level and E_f is the final energy level (see Ebbing 1996). When a projected electron strikes an atomic electron, knocking it out of place, a hole is created in the atom's electron configuration. Based on the quantum theory, which states that an inner orbital fills before an outer orbital, the hole must be filled by an outer shell electron for the atom to restabilize. Therefore, an electron of a higher energy level undergoes a transition that fills the hole and emits a photon. The system detects the emitted photon and by the wavelength or energy of the photon recognizes the element of origin.

Electrons are arranged around a nucleus in shells. A shell holds a specific number of electrons, all with the same energy level. Once a shell is full of electrons the next outer shell begins to fill. The atomic number represents the number of electrons an element has in its neutral state and implies the number of shells. The atomic number is directly proportional to the potential number of emitted photons from a single impact event (Figure 8). The multiple photon emission often results in peak overlap or complete hiding of a peak (see limitations below).

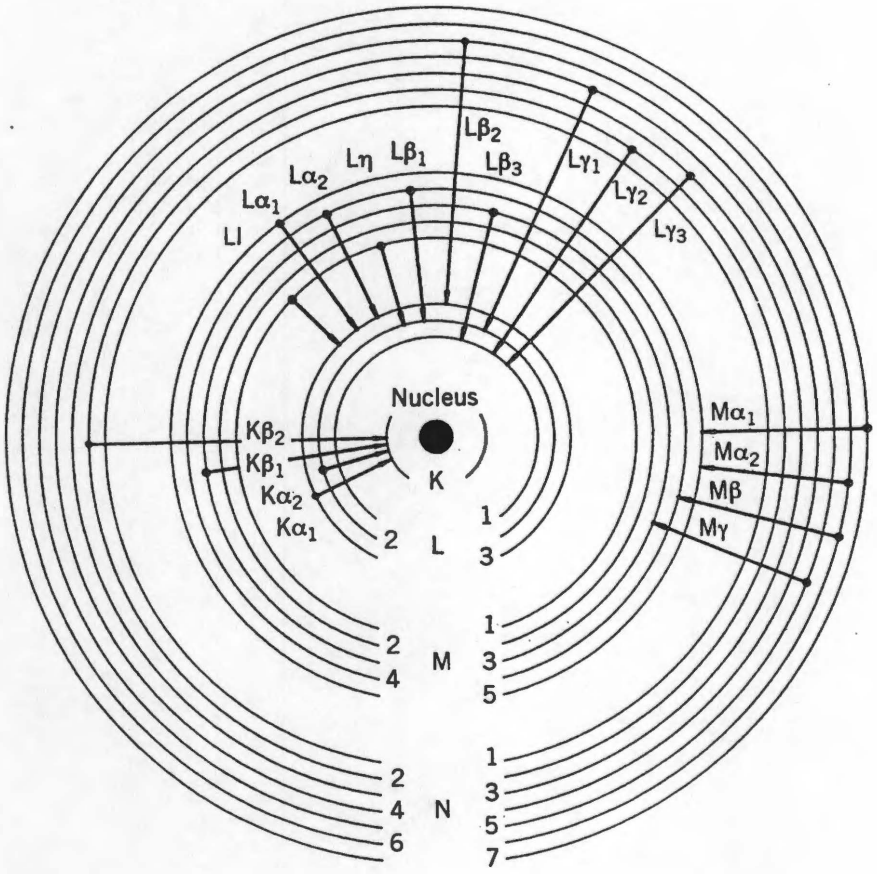

Figure 8. Possible electron transitions from single impact event to a heavy atom. K,L,M,N represent the atomic shells, each electron is arranged within an orbital (represented by the numbers) within an atomic shell at any given moment. When an electron undergoes a transition from an outer orbit to an inner orbit an energy specific X-ray is emitted (represented by the symbol above the arrow) (adapted from Klockenkamper 1997: 8).

Projected electrons that do not impact a shell electron but pass through the Coulomb field (the charged fields around the atoms) lose energy over a wide range. The X-rays generated from this interaction are white radiation or bremsstrahlung radiation that form a continuous schematic background (LeFurgey and Ingram 1990) (Figure 9). Characteristic X-rays from impact events are superimposed over the background. The background radiation often clouds the results when the peak to background ratio is nearly equal.

Principles of WDX and EDX

WDX functions by separating the X-ray of interest from the entire possible spectrum by using diffraction from a crystal. The detection of an element requires positioning the detector at the element's angle of diffraction. Because the detector blocks all emitted radiation except for X-rays from the element under investigation the peak to background ratios are excellent. Secondly, the system is sensitive to elements of low atomic number (Z), down to lithium (Z=3) (LeFurgey and Ingram 1990). However, there are several limitations of the instrument including: projecting a beam current with an intensity that severely damages biological specimens; defocusing the X-ray optic with slight movement of the beam (10-100 micrometers (μm)); and scanning for a single element at a time, missing unsuspected elements.

EDX functions by detecting, amplifying and measuring the energy of emitted X-rays. Detection occurs when an X-ray enters the lithium-drift silicon (Si (Li)) crystal. Within the crystal, the X-ray strikes atoms, losing energy but ionizing the atoms, which

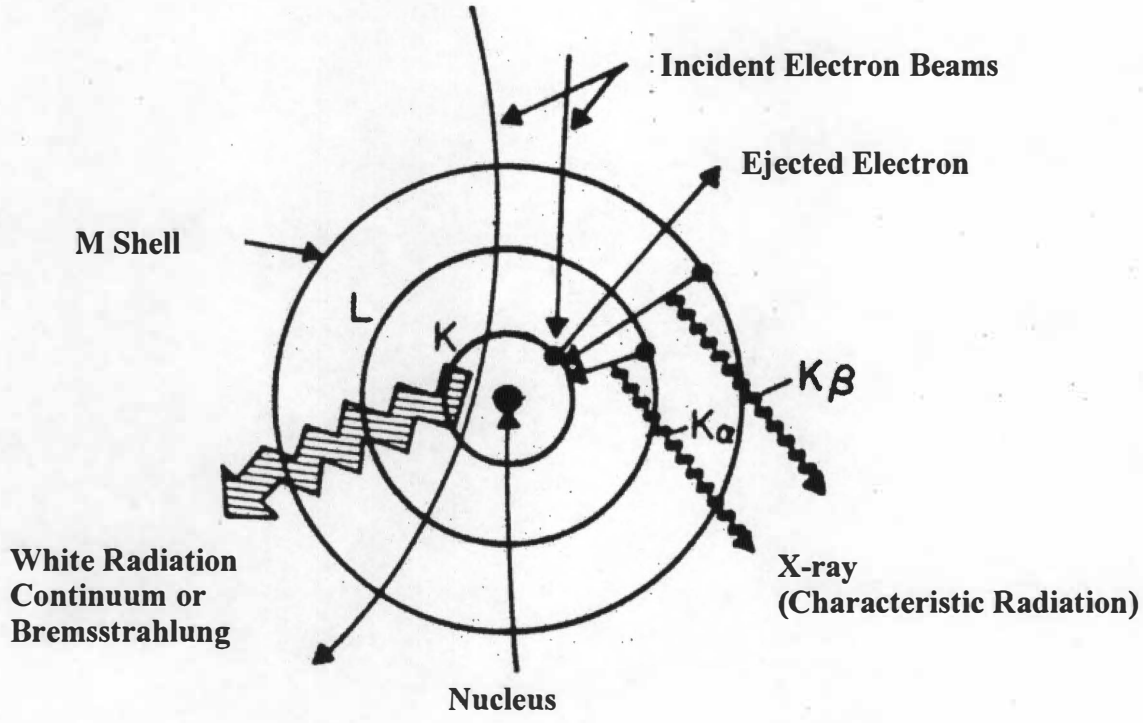

Figure 9. Possible production of X-rays. M,L,K represent atomic shells (LeFurgey and Ingram 1990: 28).

frees electrons (Figure 10). Under the influence of an applied electrical field the free electrons move towards a positively charged electrode at the rear of the crystal while the cations move towards a negatively charged surface in the front of the crystal. If all electrons reach the electrode without being trapped in the lattice imperfections or recombining the total charge is proportional to the original energy.

From the electrode, the electron charge enters a Field Effective Transistor (FET), the first stage of amplification. The FET integrates the charge and produces a small voltage step with a rise time reflecting the charge collection time, typically 10-100 nanoseconds (Russ 1984). The output continues to increase as the FET integrates charges until a point of possible non-linearity, then it shuts down and passes the pulse to the pulse processor.

Before the step-shape pulses are measured, they are further amplified and defined by the pulse processor. The conflicting functions of the processor are to produce very low noise amplification, improving peak resolution, and to handle high-count rates with efficiency. In order to reduce the noise, the pulse processor collects several signals over tens of microseconds and creates a single pulse. The detector and FET regard pulses entering microseconds apart as separate events; however, the processor's single pulse output has a magnitude equal to the sum of several of these events. After releasing the final pulse the processor returns to the baseline and begins to accept a new pulse. The pile-up pulse continues to a multichannel analyzer, which measures the final pulse and produces the schematic output.

The sensitivity of EDX analysis is compromised at every step of the system. Initially, an impact event between a projected electron and a shell electron forms a

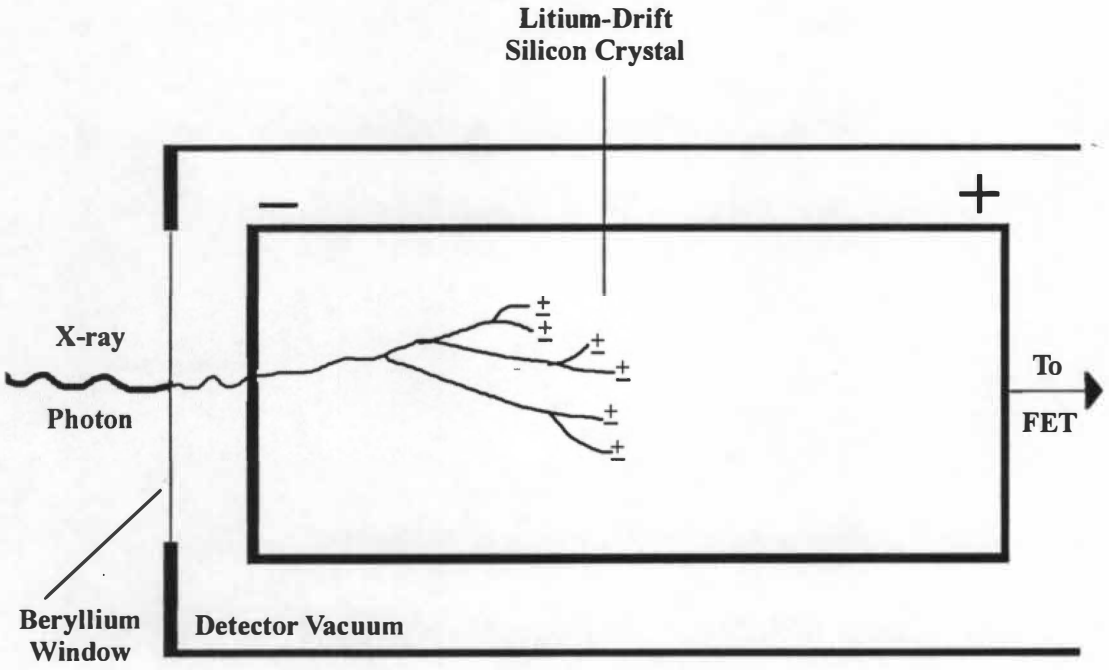

Figure 10. Schematic diagram of a Si(Li) detector used for EDX. Field Effective Transistor (FET) (adapted from LeFurgey and Ingram: 60).

number of possible transitions from one shell to another (figure 8), resulting in peak overlap. An example, potassium K_β peak at 3.59 kiloelectrovolts (keV) and calcium K_α peak at 3.69keV (LeFurgey and Ingram 1990) forms a peak overlap on the schematic output that causes an artificially high potassium peak and artificially low calcium peak. However, sophisticated computer programs have been developed for the deconvolution of such events.

Secondly, the efficiency of the detector also endangers the sensitivity of the system. In front of the Si (Li) crystal is a beryllium window. The window separated the detection apparatus from the microscope vacuum, protecting the Si (Li) crystal and excludes both low energy X-rays (less than 1keV, i.e. Na (Z=11)) and most backscatter electrons (LeFurgey and Ingram 1990). Furthermore, depletion of the Li in the crystal affects carrier mobility, slowing the arrival of some of the charges to the electrode resulting in partial measurement of the X-ray energy (Russ 1984).

In addition to the signals absorbed at the beryllium window, there are two other points in the system that signals are rejected. After the FET reaches its maximum point of pulse integration the system closes until the out-voltage returns to zero. The system can be shut down for 50-100 microseconds rejecting signals during this down time (Russ 1984). Furthermore, during the pile-up and reset time, the pulse processor rejects pulses it interprets as originating from a separate impact event.

The rejections of signals within the system, referred to as 'dead time', limits the count rate capability of the EDX system. There are several methods to correct for dead time in the system. One method includes a multichannel analyzer designed to stop the system clock while the preamplifier, amplifier, and the pulse processor are busy. It also

includes a second amplifier with a shorter integration time constant to process rejected signals. However, the fast trigger amplifier is less sensitive to lower energy signals, often unable to differentiate between them and electronic noise, and may not trigger the pulse detection circuit for them. A second method introduces a time variant circuit that changes the time constant after the peak of the pulse has passed. Initially, a long integration time is used to obtain a low noise peak. Then a very short constant quickly dumps the voltage and return to the base line, minimizing the dead time. A third method de-randomizes the incoming stream of X-rays by installing beam-blanking plates and circuits. These implements shut down the electron beam while processing a pulse and resume the beam after the processing is complete (Klockenkamper 1997).

The fundamental assumption behind the time correction methods is that counts rejected at one time can be made up at another time. This assumption is questionable especially during analysis of particles heterogeneously dispersed on a substrate. While scanning areas of high intensity, many pulses are rejected and recovered in areas of low intensity. Consequently, the total analysis is biased towards low count rate areas. Trying to remedy the problem with low integration time leads to non-recognition of lighter elements. This limitation directly affects cut mark analysis in which the residual particles are heterogeneously dispersed on the bone substrate.

Limitations of Electron Probe Microanalysis

Two properties of an element affect its delectability by electron probe microanalysis: atomic weight and quantity. Elements with an atomic number greater than 22 (titanium) are measured with air-path X-ray optics; and elements with atomic numbers

from 11 (sodium) to 22 (titanium) are measured with vacuum or helium-path optics; however, elements with atomic numbers below 11 (sodium) are not detectable by the system (Birks 1971). Furthermore, the practical limit of delectability is 100 to 500 parts per million (ppm) (Birks 1971). Elements present in lower quantities are not detected.

Ion Probe Microanalyzer

History

In 1920, Thompson observed that ions striking a metal plate caused the emission of secondary ions, mostly uncharged with a small fraction carrying a positive charge. In 1936-1937, Arnot and Milligan investigated, with the aid of a magnetic deflection field, the secondary ion yield and energy distribution of negative ions-induced by positive ions. In 1949, Herzog and Viehboeck developed the first instrument to use an electron impact primary ion source (see Benninghove et al. 1987). The construction of a complete secondary ion mass spectrometer (SIMS) followed ten years later. The first commercial SIMS produced specifically for microanalysis application was intended for analysis of extraterrestrial material brought back to earth in the beginning of the "space age". Today, investigators recognize static SIMS as an excellent instrument for surface analysis that overcomes several of the limitations of electron probe microanalyzer.

Formation of Secondary Ions

Secondary ions form from the bombardment of a specimen's surface with a primary ion beam consisting of oxygen anion and cation (O^-, O^{2+}), argon cation (Ar^+), or cesium cation (Cs^+). The bombardment results in two events: changes in the surface and

emission of particles. The energy and momentum transfers from the projected ion to a limited area and causes a change in the lattice structure and a loss of surface material by sputtering. The ion-induced emitted particles include electrons, photons and surface atoms or molecules in charged, uncharged or possibly excited states (Benninghove et al. 1987). The emitted particles of interest are the secondary ion in both the ground and exited states. These ions originate from the surface of the specimen, making the system surface sensitive. A detector attracts the ionized particles, then separates them by their mass-to-charge ratio and counts them.

There are two analytical settings of SIMS: static and dynamic. Static SIMS analyzes the composition of the upper most monolayer without disturbing its structure. The system achieves this with a very low primary ion current density (10^{-9} A•cm^{-2}, (A = the acceptance area, cm^2 = centimeters squared)) (Benninghove et al. 1987). Under this condition a monolayer has a lifetime of several hours. Dynamic SIMS applies a high primary ion current (density of A•cm^{-2}) to the surface causing the lifetime of a monolayer to decrease to 10^{-3} second (Benninghove et al. 1987). The fast surface erosion continuously moves the actual surface into the bulk providing a chemical profile of the sample.

Limitations of Ion Probe Microanalyzer

Microscopists developed SIMS to overcome the limitations of electron probe microanalysis, especially its limited detection. SIMS detects all elements and is not complicated by background radiation. Furthermore, the instrument's sensitivity to elemental concentration is dependent on analytic condition, but can range from 0.1ppm

for zinc (Zn) to 0.008 ppm for aluminum (Al) (Benninghove et al. 1987). However, a devastating shortcoming of ion probe microanalyzer is its requirement for the specimen chamber to be in the proximity of a vacuum. The porosity of bone inhibits pumping it down to this level. Furthermore, biological samples must be completely dry, without water or grease, to be accurately analyzed. Liquid and grease contaminates the detector and causes erroneous results. A final limitation of the ion probe microanalyzer, which the electron probe microanalyzer shares, is difficulty obtaining quantitative results. Both instruments require the surface of the specimen to be smooth and reflexive for quantitative analysis. The rough surface of bone traps X-rays and secondary ions so the system can not detect them, resulting in less then accurate counts.

Environmental Scanning Electron Microscope

Another advancement of electron microscopy, which has a direct impact on surface analysis of bone with electron probe microanalysis, is the environmental scanning electron microscope (ESEM). ESEM alleviate difficulties associated with pumping down porous samples to an approximate vacuum chamber by introducing a gaseous environment into the specimen chamber. It is capable of maintaining a pressure of at least 609 Pascal (Pa), which corresponds to the saturation pressure of water vapor at 273 Kelvin (K), above this pressure water can be held in its liquid phase (Baumgarten 1989; Danilatos 1991, 1993). Therefore, wet samples can remain fully hydrated, eliminating the need to desiccate a sample, a procedure that is often destructive to fragile bone.

Although the specimen chamber is a gaseous environment, the gun chamber must remain as an uncontaminated vacuum. The two chambers are separated by a series of

stages. The electron beam travels through a small aperture present in each stage. A stage specific pump maintains the required pressure gradient to stop contaminants from reaching upper chambers (Baumgarten 1989; Danilatos 1991, 1993).

A gaseous detector device (GDD) uses the gas in the specimen chamber to increase the amplification and detection of a signal. An induced moderate electrical field forces collision between the X-rays and the gas molecules. The collision causes ionization that frees electrons, similarly to ionization within the detection crystal, resulting in an increase signal (Danilatos 1991, 1993). Furthermore, the positive ions present in the gaseous environment neutralizes surface charges of insulating specimens, eliminating the need to coat these samples with reflective chemicals (Danilatos 1991, 1993).

The diameter of the electron probe affects the resolution of the ESEM. Contact between the projected electron beam and the gaseous environment scatters some of the electrons, adding to background noise. However, only a fraction of electrons is scattered, the remainders maintain the original projectory. In order to obtain the same resolution as high vacuum system the pathway through the higher pressure chambers must be short enough and the original beam must have a large enough diameter that after backscatter the resultant beam is equal in diameter to the SEM beam (Baumgarten 1989; Danilatos 1991, 1993).

In conclusion, the development of the ESEM makes EPMA accessible to wet biological samples. For surface analysis of trace elements IPMA is a better instrument; however, at the present time, it is not applicable to biological samples. For this reason, WDX and EDX are the instruments used for analyzing fresh bone. Undoubtedly, with

future advancements IPMA will replace EPMA for surface analysis of biological samples.

Chapter 3

Methods

Steps of Procedure

Three domestic pigs, *Sus scrofa*, were obtained from the University of Tennessee swine farm (Table 1). A veterinarian euthanized the pigs at the farm intravenously the morning of the experiment. The pigs were taken to the University of Tennessee Forensic Anthropological Research Facility and placed on the ground, separated by several meters. The facility is an open-air, moderately wooded experimental center bounded by a modesty fence surrounded by a chain-link fence ringed with razor wire. The flora is consistent with that of East Tennessee, but the fauna is limited to birds and rodents that may burrow under the fence. The experiment took place in mid-October and the pig carcasses remained relatively undisturbed until the beginning of January. During this time, the weather conformed to that common to East Tennessee during winter (average temperature 40 degrees Fahrenheit) (The World Almanac 1997).

The experimenter used a serrate, a slightly serrated and a smooth bladed knife (Figure 11, 12 and 13) manufactured by Tramontinal USA, Inc with stainless steel for the study (see Table 2 for metal composition). The knives chosen for the study varied only in blade type. The serrated bladed knife was an "8" Roast Slicer" from the Pulsar II

Table 1. General information and blade type assigned to on *Sus Scrofa*.

Sex	Weight (kg)	Age	Blade Type
Female	85.5	6 months	Smooth
Male	91.8	6 months	Serrated
Male	89.1	6 months	Slightly Serrated

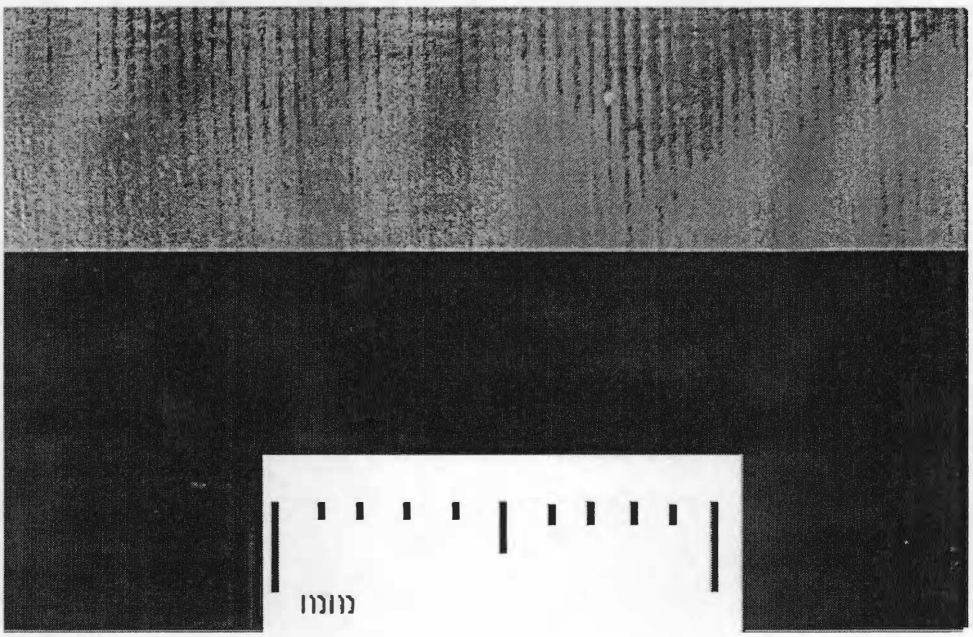

Figure 11. Smooth edge knife as seen under a dissecting microscope, 70X.

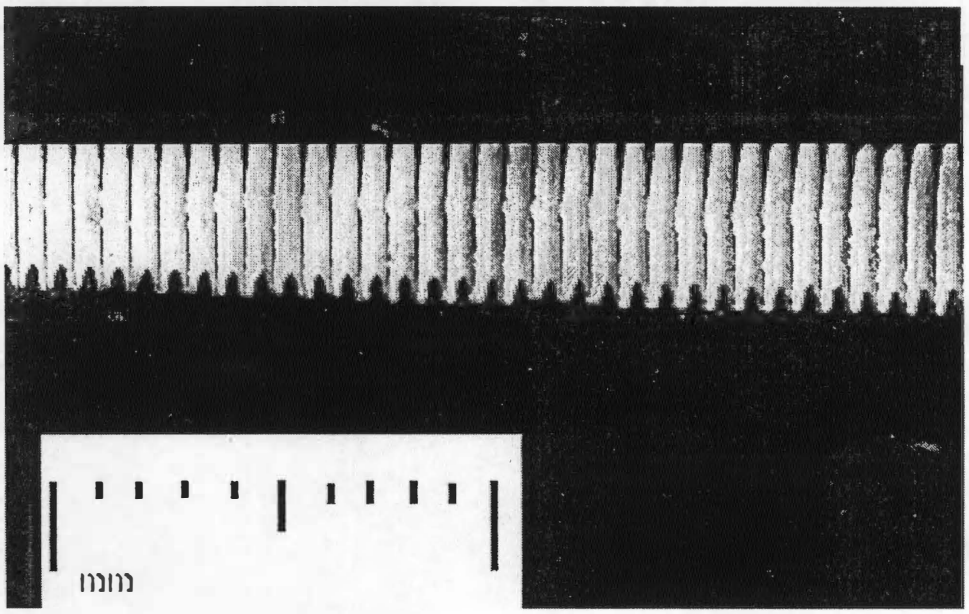

Figure 12. Slightly serrated edge knife as seen under a dissecting microscope, 70X.

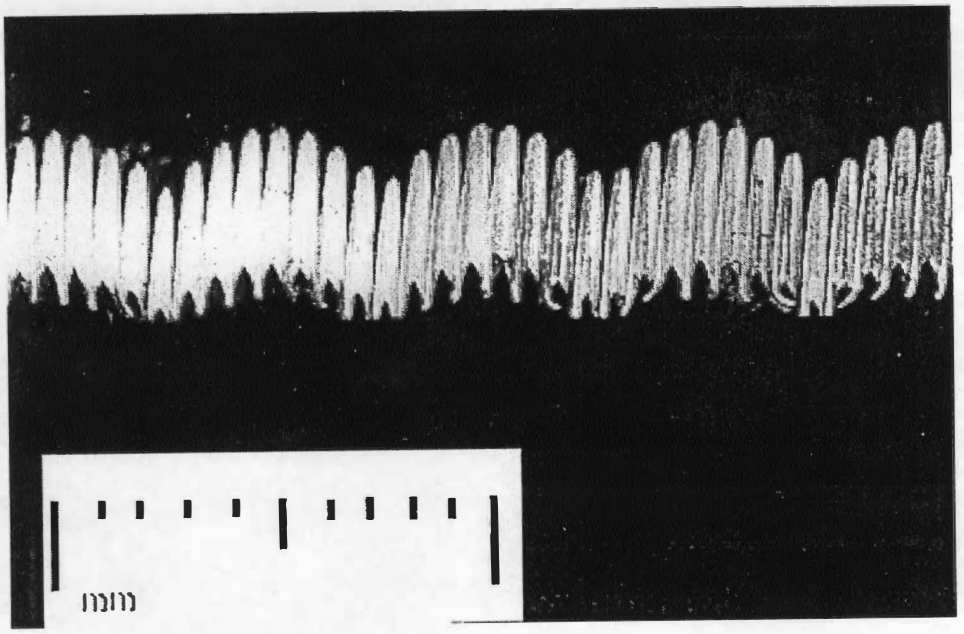

Figure 13. Serrated edge knife as seen under a dissecting microscope, 70X.

Table 2. Elemental composition of stainless steel.

Elements	Percent
Carbon	0.15-0.40
Manganese	1.00 max.
Silicon	1.00 max.
Chromium	12.00-14.00
Nickel	0.50 max.
Phosphorous	0.30 max.
Iron	83.03 min.

collection with a scalloped edge. Each scalloped edge was two millimeters (mm) in width and depth with a micro-serrated edge. The tip of the blade, top two centimeters (cm), was smooth. The slightly serrated bladed knife was an "8" Cook's Knife" from the Pulsar II collection. The blade edge was micro-serrated, but not scalloped. The tip of the blade, top 2cm, was smooth. The smooth blade was an "8" Cook's Knife" from the Old Colony collection. The blade was smooth from tip to heal.

The investigator randomly assigned a knife for each pig. A male and female experimenter stabbed each pig several times, holding the knife in an overhand grip carcass. The female experimenter stabbed the right ribs of each pig, the male experimenter stabbed the left ribs of each pig and both experimenters stab the vertebral column. Finally, the experimenters decapitated the pigs. Following the stabbing, they laid each pig on its left side for decomposition and covered it with heavy black plastic, weighted down with dirt. The black plastic shielded the pigs from direct sunlight to create an environment conducive to maggot growth. The pigs remained at the facility relatively undisturbed for two and a half months.

Recovery of the bones persisted over a four months period as the soft tissue continued to decompose. The investigator transported the bones from the facility to a laboratory in a plastic trash bag. At the laboratory, she rinsed the bones with tab water, to remove remaining soft tissue, and placed them on a drying rack for several days.

Each bone was cut to meet the size limitations of the specimen chamber of the ESEM with a Delta Bench Band Saw. The bone was then submersed into ethanol and agitated by hand for one minute. It was removed from the alcohol and dried with a heat lamp. The process was repeated. After the bone was completely dry it was placed in a plastic bag.

The experimenter randomly chose 30 cut marks from each pig, about 15 from vertebral bones, seven or eight from left rib bones and seven or eight from right ribs (Table 3 and Figures 14, 15 and 16). With Manco, adhesive-mounting putty, the bones were secured to the specimen stand to allow maneuvering inside the specimen chamber

Table 3. Number and type of bone analyzed for each blade.

Blade Type	Bone	Number of Cuts Analyzed
Smooth	Right Ribs	6
	Left Ribs	11
	Vertebrae	13
Serrated	Right Ribs	7
	Left Ribs	10
	Vertebrae	13
Slightly Serrated	Right Ribs	7
	Left Ribs	10
	Vertebrae	13

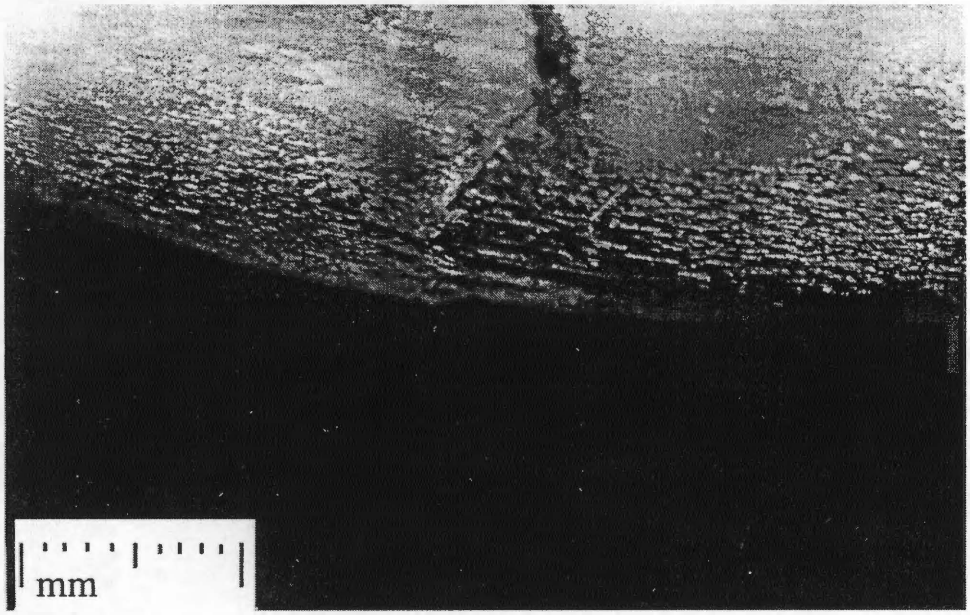

Figure 14. Cut mark inflicted by a smooth edged knife as seen under a dissecting microscope, 70X.

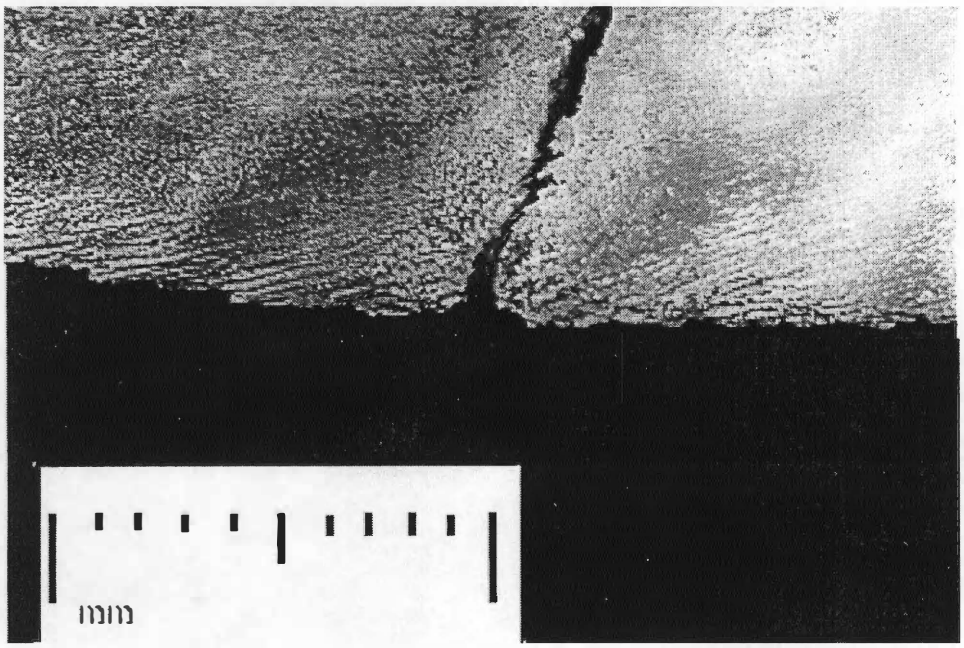

Figure 15. Cut mark inflicted by a slightly serrated edged knife as seen under a dissecting microscope, 70X.

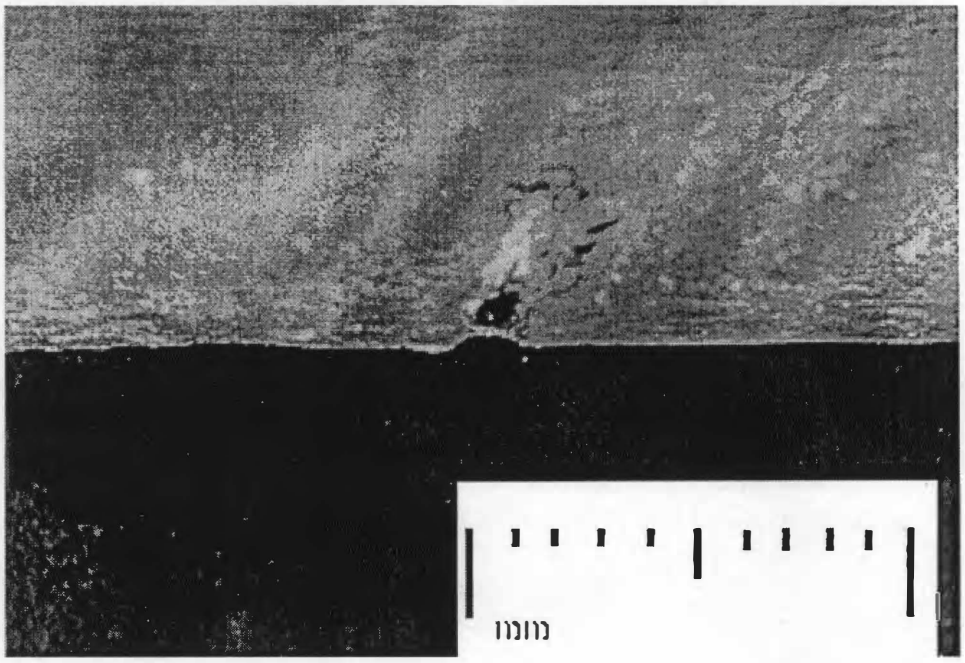

Figure 16. Cut mark inflicted by a serrated edged knife as seen under a dissecting microscope, 70X.

without the bone falling off the stand.

The investigator analyzed each bone with an Emas/mas environmental scanning electron microscope equipped with a Robinson Detector for EDX analysis (Figure 17). The specimen chamber remained at a consistent 50 Pascal (Pa) with a constant electron beam energy of 20.0 kilovolts (kV). The working distance (WD), the distance between the sample and the detector ranged from 9mm to 21mm (Figure 18). Each area was analyzed with the spot mode, which holds the beam in a single spot during analysis. The experimenter randomly pointed the gun into the cut mark and allowed the system to continue to count emitted X-rays until it registered a minimum 200 calcium (Ca) counts. The investigator then focused the beam on a control area until the Ca counts matched that of the cut mark.

The output of the system generated a schematic diagram of the elements identified with a count scale. Initial observation indicated that with matched Ca counts, only the counts of carbon (C) varied significantly (Figure 19). The author used the count scale to numerically represent the differences in the amount of C recognized.

After completion of analysis, the investigator measured the maximum depth of each cut mark using a Goldman-Fox/Williams DE Probe, manufactured by Hu-Friedy Mfg. Co., Inc. Maximum depth was defined as the maximum distance from the point of the 'V' of the cut to the outer surface of the bone (Figure 20). Cuts that completely bisected the bone were given the maximum depth measurement of 10mm.

The *t*-test and chi-square statistical tests were used to establish any significant difference in the amount of C between the cut marks and the controls. An ANOVA statistical test was used to demonstrate significant differences in the maximum depth of

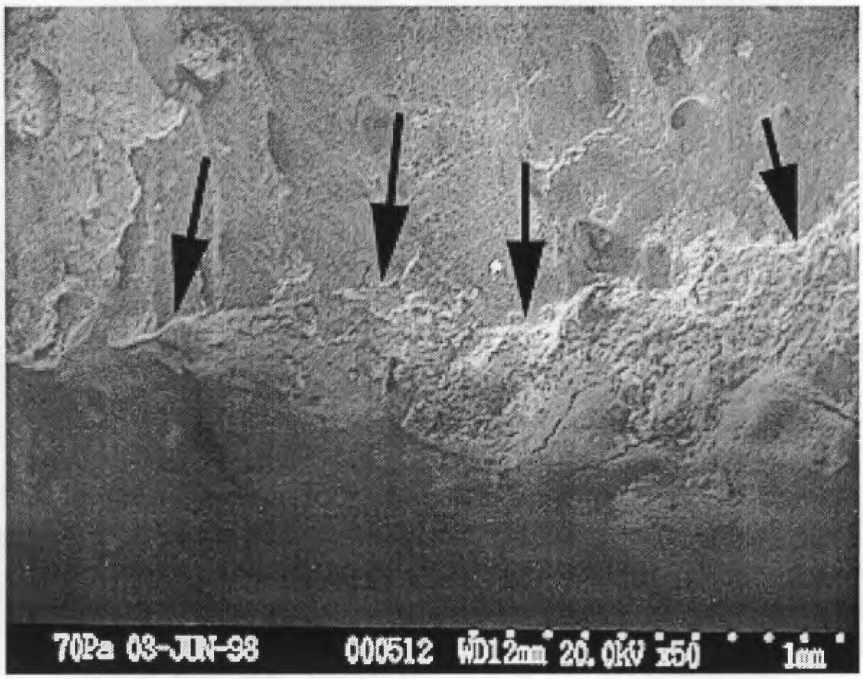

Figure 17. Cut mark as seen with the SEM at 5000X. Arrows point to edge of mark.

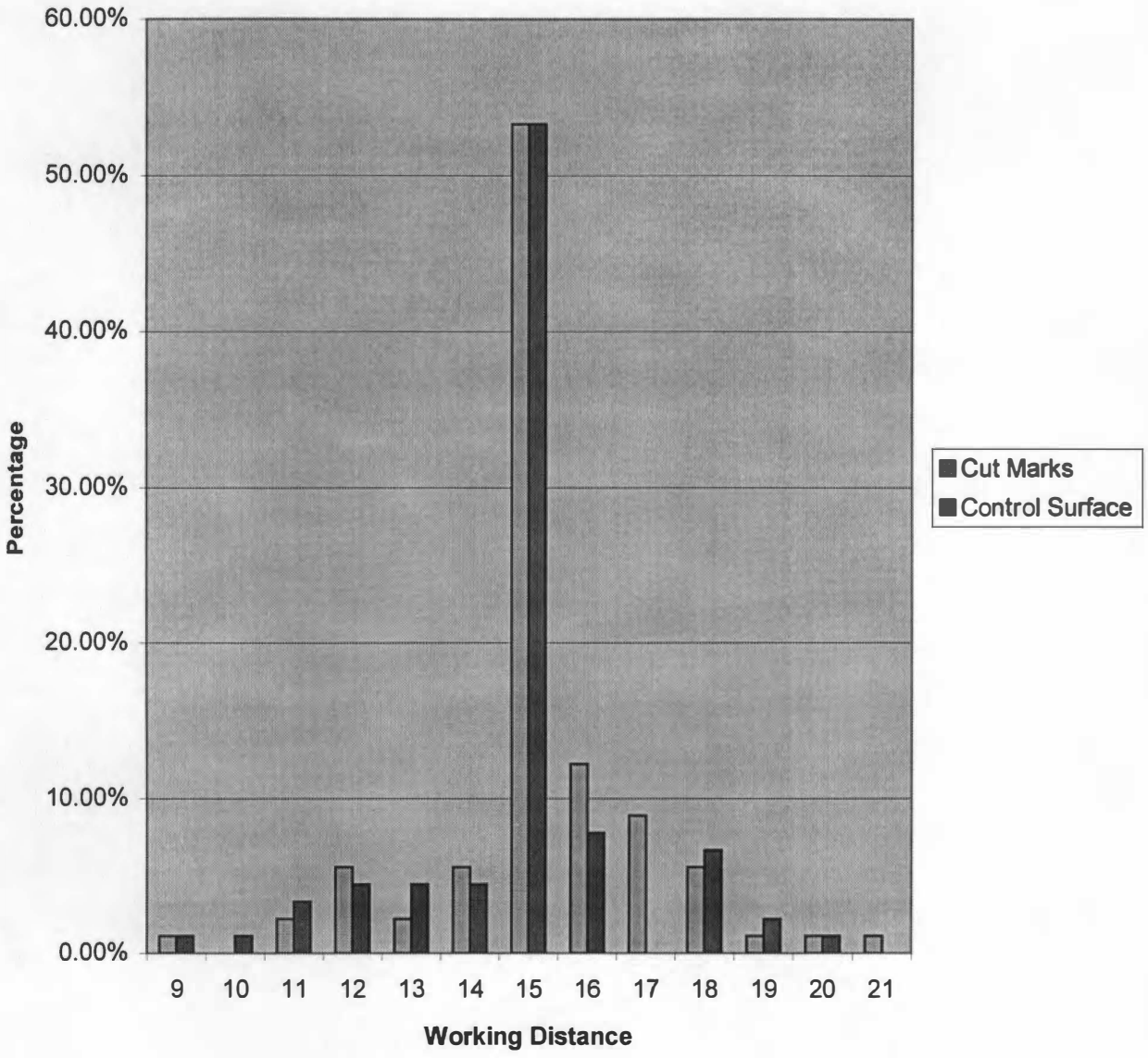

Figure 18. Distribution of working distance (WD) used to analyze cut marks and control surface.

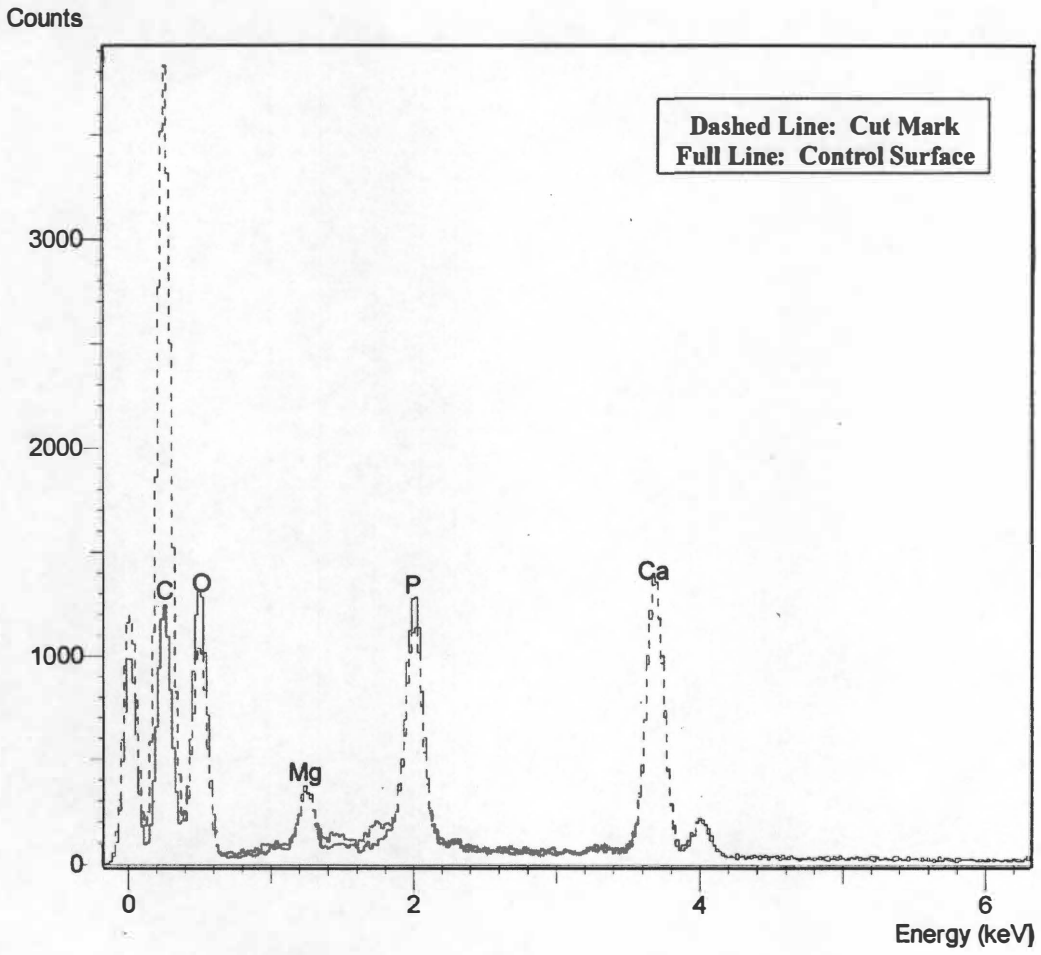

Figure 19. Schematic diagram of EDX analysis of cut mark compared to control surface.

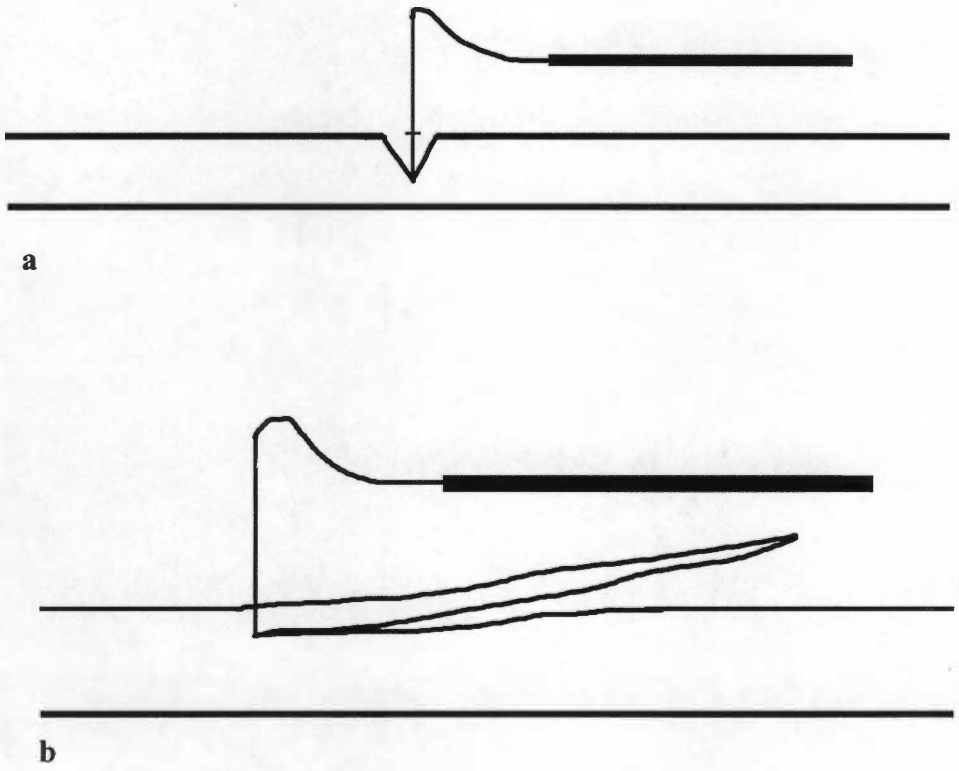

Figure 20. Orientation of DE Probe for measuring maximum depth of a) a vertical cut mark and b) an angled cut mark.

the cut mark between the three types of knives. Both were preformed using *SAS* for Windows v6.12.

Chapter 4

Results

This study compared two properties of the cut marks, maximum depth and the amount of carbon (C) measured, using several statistical tests. Each blade type was represented with a sample size of 30 cut marks that permitted the assumption of normal distribution based on the Central Limits Theorem (Ott 1993). Furthermore, each cut mark was independent of every other cut mark. These two characteristics of the sample ensure the data met several parameters (i.e., independence and normal distribution) assumed by the statistical tests.

Levine's Test

Evaluation of the variances of the means of maximum depth of the three populations was done using the Levine's Test for Homoscedasticity (Ott 1993). The null hypothesis states that the variances between the cut marks resulting from the three blade types are equal. The results of the test suggest a failure to reject the null hypothesis at the α=0.05 level (p-value 0.0636), indicating the variances of the three populations are equal.

ANOVA Test

ANOVA statistical test was used to compare the means of maximum depth of the marks of the three populations. ANOVA makes three assumptions: 1) independent observations, 2) normal distribution, and 3) equal variances (Schlotzhauer and Littell 1987). All assumptions were met. The null hypothesis stated that the mean depth of the

Table 4. Statistical results for all tests preformed.

Statistical Test	Knife types Compared*	Sample Size (N)	*P*-Value
Levine's	All Types	90	0.0636
ANOVA	sr, ss	30, 30	0.3633
	sm, sr	30, 30	0.0009
	sm, sr	30, 30	0.0258
Chi-square	sr	60	0.302
	ss	60	0.001
	sm	60	0.001
Paired *t*	sm	30	0.002
	ss	30	0.0353
	sr	30	0.5329

*sr – Serrated bladed knife, sm – Smooth bladed knife,
ss – Slightly serrated bladed knife.

three type of cut marks were equal. The results suggested rejecting the null hypothesis at the α=0.05 level when comparing all three groups. Further testing indicated a failure to reject the null hypothesis at the α=0.05 level when comparing the cut depths made with the serrated and the slightly serrated bladed knives, but to reject the null hypothesis at the α=0.05 level when comparing the cut depths resulting from the smooth and the serrated bladed knives and the smooth and the slightly serrated bladed knives (see Table 4 for p-values). Therefore, these results suggested that the means of maximum depth of cuts made with the serrated and slightly serrated bladed knives are relatively equal while the mean of maximum depth of the cuts made with the smooth blade is not similar to either.

Chi-square Test

A Chi-square test was used to evaluate the dependency of the amount of carbon (C) on the area. Since the Chi-square test treated the cut mark and control area independently the sample sized double for each blade type (n=60). The null hypothesis states that the amount of C measured was independent of the area analyzed, cut mark or control surface. The results indicated a failure to rejecting the null hypothesis for serrated bladed knife α=0.05 level, but to reject the null hypothesis for the slightly serrated bladed and the smooth bladed knives at the α=0.05 level (see Table 4 for p-values). Therefore, the amount of C measure in an area was independent of the type of area for the serrated bladed knife, but was dependent on the type of area for the smooth and slightly serrated bladed knives.

Paired Student's *t*-Test

The paired Student's *t*-test was used to define any significant difference in the amount of C measured between the cut mark and the control surface. The null hypothesis stated that the amount of C measured within the cut mark and on the control surface were relatively equal. Based on the results of the test, the investigator rejected the null hypothesis for the smooth bladed and the slightly serrated bladed knives at the α=0.05 level, but failed to reject the null hypothesis for the serrated bladed knife at the α=0.05 level (see Table 4 for p-values). Therefore, the measured amount of C found in the cut marks made with the smooth and slightly serrated bladed knives was significantly more than that measured on the control surface. However, the amount of C measured in the cut

marks made with the serrated bladed knife was relatively equal to that measured on the control surfaces.

Chapter 5

Conclusion

When presented with a forensic case the goals of forensic anthropologists include identify the individual, estimate time since death and note all ante, peri and postmortem skeletal abnormalities. Refinement and advancement of methods utilized to accomplish these goals are the aim of a large portion of forensic and physical anthropological research. Keeping with this trend, this study attempted to develop a technique for the classification of bone abnormalities, specifically cut marks.

Cut marks located on bones suggest suicide, accidental or homicidal death and are of interest to medico-legal practitioners. Because cut marks often lead to a criminal investigation, positive mark classification with a high level of confidence is imperative. Current methods of mark classification are morphologically based without an alternative method to support the results or to measure classification accuracy.

The goal of the study was to develop a cut mark classification technique based on characteristics beyond morphology. The hypothesis stated that as sharp instruments cut into bone residual material transfers from the instrument to the bone. In return, the presence of residual material within a mark would indicate the mark was the result of sharp force trauma opposed to biological agents or post-depositional processes.

Test Design

The test was designed to generate cut marks that mimic perimortem sharp force trauma. For this reason, the experimenters stabbed completely fleshed pigs,

approximately two hours after intravenous euthanization. Leaving the pigs in an open aired facility to decompose exposed them to the depositional and post-depositional processes common in many forensic cases. Furthermore, the investigator used inexpensive kitchen knives, the most common weapons utilized in sharp forced trauma (Hunt and Cowling 1991).

The test design introduced two variables into the study: blade type and force of impact. The amount of material transferred from the knife to the mark was hypothesized to be directly proportionate to the force of impact. Furthermore, a critical force, necessary for the transfer of material, was believed to exist. The critical force was unknown and the amount of force behind each blow was not measured. Two experimenters stabbed the pigs in the hope that some of wounds would be inflicted with a force greater than the hypothesized critical point.

The bones where not macerate for fear that soaking and heating them in bleach and detergent water would remove residual material. However, upon initial analysis inconsistency in the results obtained from multiple point analysis on a single bone's control surface indicated that foreign material (i.e., dust) needed to be removed from bone surface. Ethanol was chosen as the cleaning reagent after comparing elemental profiles of bones washed in it to bones washed in acetone and sterile water. The ethanol most adequately removed foreign particles without depositing any elements of interest on the surface.

Calcium (Ca) counts served as the control because it is a major component of bone, homogenous throughout the tissue, and not present in stainless steel. With the matching of Ca, nearly all other peaks matched, including oxygen, phosphorous and

magnesium (Figure 19), only the carbon (C) peaks showed a mark difference. For this reason, C counts were used to compare the elemental composition of the cut mark to the control surface. However, C was an extremely poor element to represent compositional differences between the two areas. First, C was present in both the stainless steel and the bone, and second, the percent of C in the stainless steel was very low when compared to iron (Fe) or chromium (Cr) (Table 2). If the difference in the amount of C was a result of residual material transferred from the knife then the amounts of Fe and Cr were also expected to be greater in the cut mark, but they were undetectable.

The statistical analysis indicates that significantly more C was present in the cut marks generated with the smooth and slightly serrated edged knives than on their respective controls. Meanwhile, a relatively equal amount of C was measured in the cut marks generating with the serrated edged knife as was measured on the control surface. The possible reasons for the disparity were numerous and included the manufacturing process of the knives, the release of C from the marrow cavity and limitations of EDX analysis. The manufacturing process of the slightly serrated or smooth bladed knives may have included coating the blade with C or the material of the serrated bladed knife may be harder than the material of the other knives. Furthermore, the source of the C may have been the marrow cavity. By measuring the maximum depth of penetration, the author investigated the possibility that the smooth and slightly serrated edged knives had a higher frequency of penetrating the marrow cavity, releasing carbon based organic compounds. However, the marks resulting from the serrated edged knife were not significantly more shallow. Additionally, EDX analysis is most accurate when applied to a smooth reflexive surface. In contrast, the bone samples were porous and the cut mark

created a beam-consuming crevice. Many X-rays were probably absorbed in the porosity of the bone and the depth of the cut and were not detected; therefore, absent in the elemental profile. Finally, an element must be present in an amount greater than 100ppm for detection (Birks 1971). A failure to detect a specific element suggests one of two conclusion: the material was absent or the material was present but in less than the critical quantity.

The reason the analysis was done with an ESEM equipped with EDX, despite its limitations, was because it is a relatively common instrument in research facilities. In addition to establishing a method for cut mark classification, a goal of the study was to develop a practical technique. WDX is also an accessory of ESEM and equally as prevalent; it also provides a better peak to background ratio. WDX was not used for this study because the instrument must be set to detect a specific element, a general sweep over a surface area is not possible (Birks 1971). However, since the composition of stainless steel is known the investigator did not need to fear overlooking important, but unsuspected elements; therefore, this experiment should be repeated with WDX.

The conclusion of the study is that cut marks inflicted on fleshed bones by stainless steel knives are unrecognizable by elemental composition as determined with EDX. At this time, it is unknown whether the limitation of EDX inhibited the elements of interest from being detected or if the material did not transfer from the knife to the bone during the infliction of the cut mark.

Chapter 6

Discussion

Implications of the Study

Since the birth of anthropological thought, anthropologists have used cut marks to infer human activity while hunting for diagnostic criteria for their classification (White 1992). Impressive information has been gained from visual examination of marks experimental infliction on bone (see Walker and Long 1977) and phenomenal success rate of accurate classification of experimental marks using dissecting microscopes and magnifying glasses have been documented (see Blumenschine et. al. 1996). However, as of present, no diagnostic criterion for mark classification has been defined (White 1992). Furthermore, the lack of an alternative method, one not reliant on morphologic characteristics, eliminates evaluation of classification accuracy of non-experimental marks. Meanwhile, the prevalence of forensic anthropological casework increases, as does the role of cut marks in medico-legal investigation, raising the stakes on accurate mark classification.

This thesis was an unsuccessfully attempt to develop an alternative method to classify cut marks. However, the study introduces cut mark classification to a field, electron and ion microscopy, which has the potential to provide anthropology with the necessary instruments to develop an appropriate method. WDX analysis has strength that overlaps the weaknesses of EDX analysis and may provide positive identification of elements common to stainless steel in the cut mark. In addition, advancements of IMPA are increasing the applicability of the instrument to biological studies (Benninghove et.

al. 1987). Once applicable to bone, IMPA has the potential to identify material present in extremely small quantities (0.1ppm for Zn to 0.008ppm for Al) (Benninghover et al. 1987).

In conclusion, the best methods available for cut mark classification continue to be based on morphological characteristics. Although such techniques are qualitative, efficiency and accuracy can be achieved with an adequate appreciation of skeletal variation. As illustrated by the trial involvement of Frayer and Bridgens (1985), Symes et al. (1998) and Sauer (1984) cut mark classification using morphological methods by individuals trained in skeletal biology is adequate enough to be admissible in court.

Bibliography

Adelson, I.
1974 *The Pathology of Homicide.* Charles C. Thomas Springfield, IL.

Andahl, R. O.
1978 The examination of saw marks. *Journal of Forensic Science Society* 18:31-46.

Andrews, P. and J. Cook
1985 Natural modifications to bones in a temperate setting. *Man* 20:675-691.

Baumgarten, V.
1989 Environmental SEM Premieres. *Nature* 341:81-82.

Behrensmeyer, A. K., K. D.Gordon and G. T. Yanagi
1986 Trampling as a cause of bone surface damage and pseudocutmarks. *Nature* 319:768-771.

Benninghoven, A., F. G. Rudenauer and W. H. Werner
1987 *Secondary Ion Mass Spectrometry: Basic Concepts, Instrumental Aspects, Applications and Trends.* John Wiley and Sons, New York.

Birks, L. S.
1971 *Electron Probe Microanalysis.* Second Edition. John Wiley and Sons, New York.

Blumenschine, R. J., C. W. Marean and S. D. Capaldo
1996 Blind test of inter-analyst correspondence and accuracy in the identification of cut marks, percussion marks, and carnivore tooth marks on bone surfaces. *Journal of Archaeological Science* 42:493-507.

Blumenschine, R. J. and M. M. Selvaggio
1988 Percussion marks on bone surfaces as a diagnostic of hominid behavior. *Nature* 29:21-51.

Brandes, E. E. and G. B. Brooks (Eds.)
1992 *Smithell's Metal Reference Book.* Seventh Edition. Butterworth-Heinemann Ltd. 128-129.

Bromage, T., and A. Boyde
1984 Microscopic criteria for the determination of directionality of cutmarks on bone. *American Journal of Physical Anthropology* 65:359-366.

Castaing, R. and A. Guinier
1949 Electron microscope. *Proceedings of the Delft Conference.* John Wiley and Sons, New York. p. 60.

Danilatos, G. D.
1991 Review and outline of environmental SEM at present. *Journal of Microscopy* 162:391-402.
1993 Introduction to the ESEM instrument. *Microscopy Research and Technique* 25:354-361.

During, E and L. Nilsson
1991 Mechanical surface analysis of bone: a case study of cut marks and enamel hypoplasia on a Neolithic cranium from Sweden. *American Journal of Physical Anthropology* 84:113-125.

Ebbing, Darrell D.
1996 *General Chemistry.* Houghton Mifflin Company Boston.

Fiorilo, A.
1989 An experimental study of trampling: implications for the fossil record. In (R. Bonnichsen and H. Sorg, Eds.) *Bone Modification.* Center for the Study of the First Americans, Orono, ME 61-71.

Frayer, D. and J. Bridgens
1985 Stab wounds and personal identity determined from skeletal remains: a case from Kansas. *Journal of Forensic Sciences* 30(1):232-238.

Hamperl, H.
1967 The osteological consequences of scalping. In (D. Brothwell and A.T. Sandison, Eds) *Diseases in Antiquity.* C.C. Thomas Springfield, IL. 630-634.

Hunt, A.C. and R. J. Cowling
1991 Murder by Stabbing. *Forensic Science International* 52:107-112.

Junqueira, Carlos J., Jose Carneiro, and Robert O. Kelley
1995 *Basic Histology.* Eighth edition. Appleton and Lange, Norwalk, Connecticut

Klockenkamper, R.
1997 *Total-Reflection x-ray Fluorescence Analysis.* John Wiley and Sons, Inc New York.

LeFurgey, Ann and Peter Ingram
1990 Calcium measurements with electron probe x-ray and electron energy loss analysis. *Environmental Health Perspectives* 84:57-73.

Morse, D.
1978 Ancient Disease in the Midwest. Reports of investigations No. 15. Springfield, Illinois State Museum.

Olsen, S. L. and P. Shipman
1988 Surface modification on bone: trampling versus butchery. *Journal of Archaeological Science* 15:535-553.

Ott, R. Lyman
1993 *An Introduction to Statistical Methods and Data Analysis.* Duxbury Press, Belmont, California.

Owsley, D.
1994 Warfare in coalescent tradition populations of the Northern Plains. In (D. Owsley and R. Jantz Eds) *Skeletal Biology in the Great Plains.* Smithsonian Institution Press, Washington 333-343.

Potts, R. and P. Shipman
1981 Cutmarks made by stone tools on bones from Olduvai Gorge, Tanzania. *Nature* 291: 577-580.

Reich, K. J.
1998 Postmortem dismemberment: recovery, Analysis and Interpretation. In (K. Reich Ed.) *Forensic Osteology: Advances in the Identification of Human Remains.* Springfield, IL 353-388.

Rose, J.
1983 A replication technique for scanning electron microscope: applications for anthropologists. *American Journal of Physical Anthropology* 62:255-261.

Russ, J. C.
1984 *Fundamentals of Energy Dispersive X-ray Analysis.* Butterworths & Co. Ltd.: London.

Schlotzhauer, S. D. and R. C. Littell
1987 *SAS System for Elementary Statistical Analysis.* SAS Institute Inc., Cary, NC.

Shipman, P.
1988 Actualistic studies of animal resources and hominid activities. In (S. L. Olsen, Ed) *Scanning Electron Microscopy and Archaeology.* BAR International Series, Oxford 452: 261-285.

Shipman, P. and J. Rose
1983 Early hominid hunting, butchering, and carcass-processing behaviors: approaches to the fossil records. *Journal of Anthropological Archaeological Science* 2: 57-58.

Sauer, Norman J.
1984 Manner of death: skeletal evidence of blunt and sharp instrument wounds. In *Human Identification: Case Studies in Forensic Anthropology,* edited by T.A. Rathbun and J.E.Buikstra. Charles C. Thomas: Sprinfield, IL 176-184.

Sprits, Werner U. and Fisher, Russell S.
1980 *Medicolegal investigation of Death: Guidelines for the Application of Pathology to Crime Investigation,* edited by W.U. Spitz and R.S. Fisher. Charles C. Thomas: Springfield, Il.

Symes, Steven A.
1998 Classroom discussion, April, University of Tennessee, Knoxville.

1992 *Morphology of Saw Marks in Human Bone: Identification of Class Characteristic.* Dissertation presented to the University of Tennessee, Knoxville.

Symes, S., H. Berryman and O. C. Smith
1998 Saw marks in Bone: introduction and examination of original kerf contour. In (K. Reich Ed.) *Forensic Osteology: Advances in the Identification of Human Remains.* Springfield, IL 389-409.

Walker, P. and J. Long
1977 An experimental study of the morphological characteristics of tool marks. *American Antiquity* 42(4):605-616.

White, Tim D.
1992 *Prehistoric Cannibalism as Mancos 5MTUME-2346.* Princeton University Press: Princeton, NJ.

1986 Cut marks on the Bodo cranium: a case of prehistoric defleshing. *American Journal of Physical Anthropology* 69:503-509.

World Almanac and Book of Facts 1997.
1998 World Almanac Books, Mahwah, New Jersey.

Appendix

Cut Marks Inflicted with the Serrated Bladed Knife

Bone Type	Working Dist.(mm) Cut Mark	Working Dist.(mm) Control	Pressure (Pa)	Carbon Count Cut Mark	Carbon Count Control	Maximum Depth (mm) of Cut
Right Rib	15	15	50	1700	800	2
Right Rib	15	15	50	290	270	3
Right Rib	15	15	50	3000	2100	1
Right Rib	16	16	50	1300	600	3
Right Rib	15	15	50	2700	1000	1
Right Rib	15	15	50	1500	800	1
Right Rib	15	15	50	1700	800	5
Left Rib	15	15	50	3200	8200	2
Left Rib	15	15	50	2500	600	1
Left Rib	17	17	50	5000	20000	5
Left Rib	17	17	50	3000	13000	4
Left Rib	15	15	50	3000	5800	3
Left Rib	15	15	50	2300	3300	1
Left Rib	14	14	50	3000	15000	2
Left Rib	17	17	50	4000	26000	3
Left Rib	15	15	50	5600	5600	2
Left Rib	14	14	50	9000	20000	2
Vertebra	15	15	50	3300	12000	3
Vertebra	15	15	50	900	600	2
Vertebra	15	15	50	1140	580	3
Vertebra	15	15	50	3100	1200	2
Vertebra	15	15	50	410	540	8
Vertebra	15	15	50	3100	4700	2
Vertebra	15	15	50	1200	1400	3
Vertebra	15	15	50	1600	400	2
Vertebra	15	15	50	1900	2200	2
Vertebra	15	15	50	1300	1000	2
Vertebra	16	15	50	2700	800	2
Vertebra	15	15	50	2100	1000	4
Vertebra	15	15	50	720	540	3

Cut Marks Inflicted with the Slightly Serrated Bladed Knife

Bone Type	Working Dist.(mm) Cut Mark	Working Dist.(mm) Control	Pressure (Pa)	Carbon Count Cut Mark	Carbon Count Control	Maximum Depth (mm) of Cut
Right Rib	11	17	50	1600	200	5
Right Rib	17	16	50	6200	800	5
Right Rib	12	12	50	640	100	5
Right Rib	13	13	50	2500	400	9
Right Rib	14	11	50	600	380	6
Right Rib	17	17	50	720	220	5
Right Rib	18	17	50	2500	400	3
Left Rib	16	15	50	3000	12000	3
Left Rib	18	18	50	440	440	1
Left Rib	14	14	50	1400	1600	2
Left Rib	15	15	50	2100	5700	1
Left Rib	12	12	50	1020	540	2
Left Rib	16	18	50	1500	4900	1
Left Rib	15	15	50	4000	1200	1
Left Rib	15	15	50	500	1200	10
Left Rib	15	16	50	1700	1500	2
Left Rib	15	15	50	3700	4000	1
Vertebra	9	9	50	250	130	3
Vertebra	15	15	50	1800	800	3
Vertebra	15	15	50	4100	1700	1
Vertebra	16	15	50	1500	900	2
Vertebra	15	15	50	700	300	5
Vertebra	12	12	50	280	250	2
Vertebra	15	15	50	3800	1300	1
Vertebra	16	17	50	700	360	1
Vertebra	15	15	50	2300	1600	3
Vertebra	15	15	50	3000	800	1
Vertebra	17	16	50	900	400	5
Vertebra	15	15	50	2200	100	1
Vertebra	15	13	50	900	1600	3

Cut Marks Inflicted with the Smooth Bladed Knife

Bone Type	Working Dist.(mm) Cut Mark	Working Dist.(mm) Control	Pressure (Pa)	Carbon Count Cut Mark	Carbon Count Control	Maximum Depth (mm) of Cut
Vertebra	16	16	50	18000	10000	2
Vertebra	18	18	50	2400	1200	3
Vertebra	15	15	50	2200	1100	1
Vertebra	15	15	50	1000	2800	3
Vertebra	15	15	50	10600	9000	1
Vertebra	15	17	50	460	450	1
Vertebra	15	15	50	1020	540	5
Vertebra	16	16	50	51000	11000	2
Vertebra	16	15	50	500	700	1
Vertebra	16	16	50	1000	560	5
Vertebra	15	18	50	720	820	4
Vertebra	16	15	50	104000	10000	3
Vertebra	15	15	50	1900	1300	1
Right Rib	14	14	50	4900	1500	2
Right Rib	11	10	50	1700	400	3
Right Rib	15	15	50	2100	400	2
Right Rib	15	15	50	3800	2900	2
Right Rib	15	15	50	2600	500	3
Right Rib	20	19	50	1600	300	2
Right Rib	19	19	50	1200	400	3
Right Rib	18	18	50	2200	600	2
Right Rib	17	11	50	2900	200	8
Right Rib	12	11	50	700	200	2
Right Rib	12	12	50	1600	400	3
Left Rib	15	15	50	4100	2800	2
Left Rib	15	13	50	80	210	2
Left Rib	21	20	50	600	4900	2
Left Rib	17	17	50	2400	5600	2
Left Rib	13	13	50	5600	2000	4
Left Rib	18	18	50	3600	4400	3

Vita

Jennifer Cheryl Love was born in Pittsburgh, Pennsylvania. In June of 1990, she graduated from Lakeland Senior High in Lakeland, FL. She attended Pennsylvania State University, majored in Anthropology and received a Bachelor's of Arts degree in May of 1994. She attended the University of Tennessee and received a Master's of Arts in the field of Anthropology in May of 1999.